Near ambient N_2 fixation on solid electrodes versus enzymes and homogeneous catalysts

Olivia Westhead[1], Jesús Barrio[1], Alexander Bagger[2,3], James W. Murray[4], Jan Rossmeisl[2], Maria-Magdalena Titirici[3], Rhodri Jervis[5], Andrea Fantuzzi[2]*, Andrew Ashley[6]*, Ifan E.L. Stephens[1]*

[1]Imperial College London, Department of Materials
[2]University of Copenhagen, Department of Chemistry
[3]Imperial College London, Department of Chemical Engineering
[4]Imperial College London, Department of Life Sciences
[5]University College London, Department of Chemical Engineering
[6]Imperial College London, Department of Chemistry

*email: a.fantuzzi@imperial.ac.uk, a.ashley@imperial.ac.uk, i.stephens@imperial.ac.uk

Abstract:

The Mo/Fe nitrogenase enzyme is unique in its ability to efficiently reduce dinitrogen to ammonia at atmospheric pressures and room temperature. Should an artificial electrolytic device achieve the same feat, it would revolutionise fertilizers and even provide an energy dense, truly carbon-free fuel. This Review provides a coherent comparison of recent progress made in dinitrogen fixation on (i) solid electrodes, (ii) homogeneous catalysts and (iii) nitrogenases. Specific emphasis is placed on systems for which there is unequivocal evidence that dinitrogen reduction has taken place. By establishing the cross-cutting themes and synergies between these systems, we identify viable avenues for future research.

[H1] Introduction

The triple bond in N_2 is extremely strong (941 kJ mol^{-1}). Remarkably, the nitrogenase enzyme can naturally catalyse N_2 scission at room temperature and atmospheric pressure. At ambient pressure, the Faradaic efficiency (the proportion of electrons which go towards making the desired product) of nitrogenase is 66%, while at elevated pressures (50 atm) nitrogenase can reach 75% via the reaction

$$\mathrm{N_2 + 8H^+ + 16MgATP + 8e^- \rightarrow 2NH_3 + H_2 + 16MgADP + 16}P_i, \qquad 1$$

where ATP (adenosine triphosphate) provides the energy for the reaction by transforming to ADP (adenosine diphosphate) and Pi (inorganic phosphate)[1–3]. The naturally high Faradaic efficiency of nitrogenase has inspired the development of homogeneous molecular catalysts which imitate its catalytically active centre. Ammonia is produced industrially via the Haber-Bosch process, where atmospheric nitrogen and hydrogen, derived from methane steam reforming, are combined at high temperatures and pressures (300-500°C, 100-300 atm) in the presence of a promoted Fe or Ru catalyst. The high demand for ammonia as a fertiliser means that it is produced in prodigious quantities; approximately 175 million tonnes are produced per year[4,5]. The extensive CO_2 emissions from the methane steam reforming process, as well as the extreme catalytic operating conditions, mean that this process is responsible for 1% of global energy consumption and 1.4% of global CO_2 emissions[6,7]. There is also increasing interest in ammonia's potential as a carbon-free fuel. Multiple shipping are companies already moving to ammonia-based propulsion[8], yet to be truly carbon-free ammonia production must be decoupled from fossil fuels. Thus, the catalysis of N_2 to NH_3 in

an electrolyser at low temperatures (under 100 °C) and near atmospheric pressures has gathered widespread attention. This method could be powered by renewable electricity with hydrogen supplied through water oxidation, which would be carbon-free. NH_3 could also be produced on-site and on-demand, limiting the challenges associated with its transport from a Haber-Bosch facility to a given consumption point[4,9].

An efficient N_2 reduction electrocatalyst must sustain high and stable current densities with low overpotential (η, any excess applied voltage due to kinetic factors) and high selectivity towards N_2 reduction versus H^+ reduction ($2H^+ + 2e^- \rightarrow H_2$). The US Department of Energy cite blanket performance targets of 90% Faradaic efficiency and 300 mA cm^{-2} current density (normalised on a geometric basis) for practical electrochemical ammonia synthesis[10]. High current densities are important – regardless of the final application – to minimise capital costs. However, the metrics of selectivity and overpotential have varying importance depending on the use of ammonia. Singh et al. estimated that the power needed to produce ammonia for fertilizer for a standard field (100 kg NH_3 $hectare^{-1}$ yr^{-1}) at an overpotential of 1V and 100% Faradaic efficiency would be 145 W $hectare^{-1}$. Reducing the Faradaic efficiency to 1% would increase the electrode area required for ammonia synthesis 100-fold, showing that selectivity is the limiting factor for fertiliser[11]. For the use of ammonia as an energy vector, overpotential becomes more important. If ammonia were produced at zero overpotential, the cost based on electricity prices would be comparable to that of methane. However, production at 1 V overpotential would increase prices by approximately 190%[12], making the method unviable. Stability is also a key issue; an industrial catalyst must be able to sustain a significant number of turnovers to be commercially viable.

The rigorous quantification of the often low concentrations of produced ammonia is one of the greatest problems with nitrogen reduction on solid electrodes[13]. To date, few published works have carried out this quantification successfully, while a majority of reports are false positives based on contamination[14,15]. Some of the most cited articles have been retracted, such as the report by Licht et al. published in *Science* in 2014 where nitrogen reduction was claimed to have been achieved in molten hydroxide suspensions[16]. This difficulty can also be observed in homogeneous and enzymatic nitrogen reduction. Inappropriate testing methods, such as the widely used spectrophotometric indophenol blue method, provided false positives due to the interaction with phosphine ligands in molecular catalysts[17]. Mackellar et al. (2016) further demonstrated how *Streptomyces thermoautotrophicus* UBT1 (which contains an alleged oxygen-sensitive nitrogenase enzyme) fails to incorporate isotopically labelled (15-N) N_2 gas[18], meaning that it cannot reduce nitrogen to ammonia. Schrock and co-workers were among the first to use isotopic labelling when employing molecular catalysts[19], laying the groundwork for the now widely accepted use of isotopic labelling in homogeneous catalysis. This methodology was later adopted in the rigorous protocol defined by Andersen et al. in 2019, which culminates in an isotopically labelled nitrogen reduction step[20], which is critical to ensure unequivocal ammonia production. However, it is still imperative to remove contaminants from the isotopically labelled gas, a step often overlooked in the literature[21]. This review will focus only on reports that have rigorously verified their production of ammonia. In particular, we will place specific attention on the lithium-mediated nitrogen reduction paradigm when considering solid electrodes, given that this was the one system able to pass Andersen et al.'s protocol[20,22,23].

[H2] Differences between the three paradigms

To date, no synthetic system operating at ambient temperature and pressure out-performs nitrogenase across all metrics of stability, efficiency, activity and overpotential (Figure 1 b-d). Nitrogenase hydrolyses at least two ATP molecules per electron transferred in its nitrogen reduction reaction scheme. This results in a limiting operating potential — i.e. when all elementary electron transfer steps are downhill in free energy [24]—of -0.79 V vs RHE[25], which constitutes a moderate overpotential; the standard potential for nitrogen reduction to ammonia is 0.057 V vs RHE (See SI and figure 1 b-d). It is important to note that this value allows us to compare the energetics between the three paradigms. Nitrogenase is unique in that it is able to dynamically tune operating potentials throughout the course of its nitrogen reduction scheme by accumulating reducing units[26], protein conformational changes, and complex formation[27]. Nitrogenase also exhibits remarkable selectivity towards N_2 reduction, with Faradaic efficiencies of 66% at ambient pressure[3,19,28]. Typical Faradaic efficiencies exhibited by solid electrodes do not exceed 35% at ambient pressure, and the overpotential is limited to large values (>2.5 V) by the requirement for in-situ plated lithium as a catalyst[29,30]. Homogeneous catalysts can achieve comparable, or even improved[31], Faradaic efficiencies to nitrogenase, but their per-site activity and long-term stability is often lacking. Most homogeneous systems also fail to achieve an overpotential as low as nitrogenase. All systems fall short of the 'ideal electrode', which has negligible overpotential, 100% Faradaic efficiency and a lifetime of at least 5 years (Figure 1 b-d).

To understand the differences in activity for nitrogen reduction between solid electrodes, molecular catalysts and nitrogenase, it is important to consider the mechanisms governing catalytic reactions in the three systems. Molecular catalysts can be specifically designed with fine control over the active site, activity, and selectivity due to their well-defined nature. Metal surfaces, however, are often made up of a number of different facets, geometries and structures, making it difficult to pinpoint and tune the active sites in the same way[32]. There are major differences between how electron transfer occurs in molecular complexes and enzymes versus metallic surfaces[33]. In metals, electrons are always freely available and proton and electron transfer are typically coupled, whereas the choice of reducing agent and proton donor in molecular complexes and enzymes can alter the protonation and reduction scheme followed by the catalyst, with steric hindrance providing a boost to selectivity[34,35]. Enzymatic nitrogen fixation also benefits from the dynamic environment within which it resides. The nitrogenase enzyme undergoes a number of different structural rearrangements during each catalytic cycle, allowing it to alter its kinetic and thermodynamic state [36,37]. Metallic surfaces, do not exhibit this variability. Electron screening effects mean that long-range effects can be neglected, and active sites are generally restricted to individual, static features, such as a step or edge defect, on a metallic surface[38,39]. Even though solid metal electrodes restructure under reaction conditions[40,41], it is not expected that the active sites within a pure metal catalyst structure will reversibly change during each catalytic cycle.

The working mechanism of N_2 reduction varies across enzymes, molecular complexes and solid surfaces. Nitrogenase breaks the N_2 triple bond through the polarization of the N_2 molecule by neighbouring S-H groups[28,42], with subsequent controlled protonation through the Lowe-Thorneley scheme occurring via a chain of water molecules within the anhydrous and hydrophobic environment surrounding the catalytic cofactor[43,44]. Molecular complexes, typically Fe or Mo based, can also weaken and cleave the triple N_2 bond to form nitrides,

converting N_2 into a redox-active ligand[45]. Solid surfaces can reduce nitrogen to ammonia via several different mechanisms, either associatively or dissociatively. In the majority of cases, the most energy intensive step is the breaking of the dinitrogen triple bond[46,47], which occurs spontaneously in the lithium mediated mechanism. A summary of the reduction schemes is shown in figure 2.

Scientific progress could be achieved by combining the strengths of the three paradigms. For example, the nitrogenase enzyme exhibits excellent selectivity and activity towards nitrogen reduction, as well as an intricate mechanism controlling the delivery of protons and electrons to the active site, but it occupies a much larger area than its counterparts. While the MoFe protein of the nitrogenase enzyme has a footprint of approximately 40 nm^2 [48,49], molecular complexes are often much smaller (on the order of a few nm^2), and a model metallic atom such as Ru has a diameter of 0.26 nm (Figure 1 a)[50]. If the per-site activity and selectivity of nitrogenase could be achieved on a metallic electrode, the abundance of catalytic sites would result in a current density of 7 mA cm_{geo}^{-2} (normalised according to microscopic surface area; see supplementary information)[51].

[H1] Nitrogenase

The nitrogenase enzyme performs the most consistently across metrics of stability, activity and selectivity at ambient temperature and pressure, as shown in figures 1b to d[37]. There are three known variants of nitrogenase, each defined by the metallic content of their catalytic cofactor. The most common, and most extensively studied, is molybdenum nitrogenase, which contains a [Mo:7Fe:9S:C]:homocitrate cluster as its catalytic cofactor (FeMo-co) contained within a MoFe protein[52]. The two other variants are vanadium nitrogenase, containing an FeV-co, and iron-only nitrogenase, containing an FeFe-co[52,53]. The properties of vanadium and iron-only nitrogenase are discussed in detail elsewhere[54]. This review will focus on molybdenum nitrogenase, which is the most selective of the three[55–57].

[H2] Active centre

The nitrogen reduction scheme in molybdenum nitrogenase (eqn 1.) requires 8 electron transfers and 16 ATP hydrolysis events to form 2 molecules of ammonia and an obligatory H_2 molecule[58]. Experimental data and DFT calculations suggest that the Fe atoms in the FeMo-co are the active site for N_2 binding with little evidence suggesting that any substrate or intermediate binds to the Mo atom[37]. Instead, similarly to many other biological systems, the Mo serves to provide maximal anti-ferromagnetic coupling in the FeMo-Co, which allows two iron atoms be highly reduced[36] and so able to bind N_2[36,37,43]. The central carbon atom provides structural stability, while the surrounding sulfur atoms protect the iron core from undesirable side reactions[70] as well as providing hydrogen binding sites[43].

[H2] Transport of reactants

One of the most surprising aspects of nitrogenase is its high selectivity towards nitrogen reduction, rather than hydrogen evolution. In the absence of N_2, MoFe nitrogenase will reduce protons to evolve hydrogen[53]. However, in the presence of N_2, the hydrogen evolution reaction is suppressed, apart from the obligate release of one H_2 molecule[53]; a feature unique to nitrogenase. Nitrogenase achieves this primarily through its control over the transport of reactants, namely protons and electrons, to the catalytically active site.

Control of protons to the FeMo-co is critical. Electrochemical studies where an isolated FeMo-co had unlimited access to protons resulted in preferential hydrogen evolution[44]. Therefore the protein environment of the cofactor must deliver protons for the reaction in such a way that they can avoid recombination with electrons to form H_2[44]. The amino acid residue chains surrounding the FeMo-co shield it from water, meaning that there are no water molecules near the iron atom active sites. There is also evidence of hydrophobicity in the immediate environment of the FeMo-co, meaning that the active site for nitrogen binding exists in an anhydrous and hydrophobic environment[43], as shown in figure 3 b. Therefore, protons must be delivered to the FeMo-co in a controlled fashion. X-ray crystallography and molecular dynamics studies have been able to identify various channels within the MoFe protein through which substrates could be delivered to the cofactor surface[59,60]. One such channel is a water channel, suggested to permit controlled protonation of the cofactor[44]. Protons could be shuttled one at a time to the FeMo-co along a proton wire made up of eight water molecules from a proton bay via a Grotthuss mechanism[43,61], shown schematically in figure 3 c. Once an electron is transferred to the cofactor, the final water molecule releases a proton to the cofactor site[62]. All three nitrogenases contain a proton wire, suggesting that controlled protonation is key to nitrogenase functionality. Furthermore, mutant studies which impaired the functionality of the water chain, causing the proton wire to function less efficiently, severely impacted nitrogen reduction activity[43].

The Lowe-Thorneley scheme, developed in the 1980s, lays out a detailed kinetic scheme for nitrogen reduction at the FeMo-co based on the stepwise delivery of electrons and protons to the cofactor[63] (figure 3a). Electron transfer is carried out via two iron-sulfur metallic clusters (the F-cluster in the Fe protein and the P-cluster in the MoFe protein) which deliver electrons from the Fe protein to the MoFe protein and then to the FeMo-co[51]. The MoFe protein is composed of two symmetric αβ units, each of which contains a P-cluster and an FeMo-co[26]. The Fe protein, bound to two MgATP molecules, binds to each αβ unit. While ATP hydrolysis and electron transfer are clearly linked, the exact role of ATP hydrolysis and the order of events is unknown. There is evidence to suggest that ATP hydrolysis is necessary to provide the energy to transfer the electron from the F-cluster in the Fe protein to the P-cluster in the MoFe protein, the view taken in initial nitrogenase studies[64,65]. In this model, Fe protein dissociation is the rate limiting step[58]. Another model, known as deficit spending, suggests that electron transfer occurs first from the P-cluster of the MoFe protein to the FeMo-co, then an electron is transferred from the F-cluster of the Fe protein to the P-cluster to make up for the one that was lost. ATP hydrolysis then occurs after electron transfer[27]. In this model, the ATP hydrolysis instead provides the energy for the dissociation of the Fe and MoFe proteins at the end of the cycle[65]. Recent work also suggests that P_i release is the rate limiting step in the deficit spending electron transfer model[65,66].

It could be that the mode of electron transfer is dynamic, with different mechanisms taking place at different parts of the nitrogenase reduction scheme according to the transfer requirements of the intermediate nitrogenase state. Indeed, slow electron transfer is crucial for selective nitrogen reduction at step E_4 of the Lowe-Thorneley scheme, as shown in figure 3d. If there were an abundance of electrons at the FeMo-co, the reduction scheme would proceed via Coupled Proton Electron Transfer (CPET), allowing the cofactor to take the much more energetically favourable path to hydrogen evolution. Instead, a single electron transfer allows the cofactor to become reduced enough to bind N_2[37]. Indeed, kinetic studies by

Hoffman, Seefeldt and coworkers suggest that increasing electron flux to the catalytic cofactor results in a loss in selectivity for nitrogen reduction under 1 atm N_2[67]. One possible mechanism by which nitrogenase controls the access of electrons to the catalytically active site could be conformational gating. This is where an 'electron gate' in the MoFe protein can be reversibly opened and closed to control electron transfer to the active site [58]. Such conformational changes have been characterised via small-angle X-ray scattering and EPR[26].

Oxygen exposure is highly destructive for nitrogenase. The low potential iron-sulfur clusters, critical for electron transfer and catalysis, are vulnerable to oxidation which can either render them bio-unavailable or cause them to decompose[68]. The one report of a completely oxygen-resistant nitrogenase type has been disproved[18]. Many nitrogen fixers are therefore obligate anaerobes or microaerobes. One protective mechanism used by *Azotobacter* species is the formation of a ternary complex between the MoFe and Fe proteins, and another small protein, the FeSII or Shethna protein. The formation of this complex is controlled by the redox state of the [2Fe-2S] cluster contained within[69], suggesting that the role of electron transfer in nitrogenase may be even more complex.

It is clear from this discussion that the careful combination of the slow and controlled delivery of protons and electrons to the catalytically active site, as well as the exclusion of deleterious molecules such as oxygen and water, is, to a large part, what allows nitrogenase to function so efficiently.

[H2] Thermodynamic vs kinetic perspectives

Stage E_4 in the Lowe-Thorneley scheme represents a critical point. Either the cofactor returns to its original state, E_0, by the release of two H_2 molecules, or it can release one H_2 molecule and bind a N_2 molecule[28]. A mystery of this step was the obligate release of an H_2 molecule, as this seemingly wastes the energy required for 2 electron transfer steps[70,71]. Electron-Nuclear Double Resonance (ENDOR) spectroscopy of the freeze-trapped E_4 state revealed that it is contains two hydrides which bridge two Fe ions, thus forming two [Fe-H-Fe] fragments[72], as well as two sulfur bound hydrogen ions[28]. The bridge-bound hydrogen atoms have an important stabilizing function since they are less prone to further protonation, releasing H_2, than the terminal bound hydrogen to the sulfur atoms. This stability means that they are less likely to return the cofactor to its original E_1 state[73]. This evidence that nitrogenase stores electrons as hydrides provides an answer to the question of how it is able to undergo four reduction steps at constant potential when it is already fully saturated[37,74]. Additionally, the reductive elimination of these two adjacent hydrides to form H_2 leaves the metal site in a state that is doubly reduced and so able to bind and activate N_2[28,70]. The release of H_2 is also highly thermodynamically favourable, whereas the formation of a E_4(NHNH) is highly unfavourable. By combining these two processes, the overall reaction becomes downhill in energy, as shown in figures 3d and 3e [70,73].

The structure of state E_4 also ensures N protonation over Fe hydride formation via a 'push-pull' mechanism. The iron centre, having lost two hydrogen atoms, is doubly reduced and 'pushes' electron density away, which is simultaneously 'pulled' towards the N_2 molecule by the S-H group. This biases the $Fe - N \equiv N$ unit such that N protonation is favoured over protonation of the reduced Fe atom, as demonstrated by the downhill energy step in figure 3e from E_4 to E_5[28,42]. This is interesting, since normally adsorption and desorption steps are

considered separately. Yet, in the case of nitrogenase there is a concerted mechanism where the two steps occur simultaneously, without leaving an open site.

Recent DFT studies suggest that, in order to accumulate the reducing equivalents and protons required to reach state E_4, nitrogenase also employs a kinetic mechanism to avoid deleterious hydrogen evolution[75], shown schematically in figure 3 e. The E_2 state is doubly reduced, with one electron being stored as a bridging hydride and one as a reduced metal-ion core. To move to stage E_3, the cofactor must be further protonated. However, this is likely to result in hydrogen evolution and a return to the E_0 state rather than a continuation along the scheme. Instead, the S2B atom dissociates from the cofactor as an H_2S group, exposing the Fe core which can be further reduced to the E_4 state, such that the S2B atom is replaced by two neighbouring hydrides. Once the N_2 molecule has been bound, the S2B atom returns to the cofactor to allow for the final NH_3 desorption, as shown in figure 3a[37].

[H2] Key unanswered questions on enzymes

Despite the fact that the research into the nitrogenase enzyme and how it achieves efficient nitrogen reduction has been ongoing for over 150 years[28], there remain many unanswered questions. Although steps forward have been made in understanding the mechanism of electron transfer in nitrogenase, the exact order of events is disputed, as well as the true role of ATP hydrolysis[26]. In addition, the mechanism for nitrogen reduction itself is disputed. While most literature considers an associative alternating or distal scheme, the intermediates which would allow researchers to distinguish between the two have not yet been detected due to the difficulty in isolating intermediate states for analysis. This is in part due to the fact that the isolated catalytic cofactor is incapable of nitrogen reduction, and so separating the mechanism at the active site from its surroundings is difficult[75]. It is key to understand the mechanism by which nitrogenase makes ammonia, as well as how the surroundings influence this, to mimic it successfully. There have, however, been a great many steps forward in understanding; the atomic and electronic structure of the Fe-Mo cofactor have been well characterised using X-ray diffraction and Electron Paramagnetic Resonance (EPR) studies[36], and several key nitrogenase catalytic intermediates have been trapped and characterised[28]. Such breakthroughs are encouraging for future gains in understanding.

[H1] Homogeneous catalysts

Research into transition metal complexes for nitrogen reduction has been on-going since the 1960s[76]. The isolation of $[(NH_3)_5Ru(N_2)]^{2+}$ by Allen and Senoff[77] in 1965 confirmed that N_2 can coordinate as a ligand to a transition metal. However, the first successful reduction of nitrogen to ammonia at ambient temperature and pressure by a transition metal complex was not achieved until 2003. This was the seminal work of Yandulov and Schrock, who synthesised a Mo based complex containing tetradentate triamidoamine ligands[19]. Yandulov and Schrock were able to isolate metal-ligand complexes of [HIPTMo] (HIPT = hexa-iso-propyl-terphenyl, 3,5-(2,4,6-i-$Pr_3C_6H_2)_2C_6H_3$) proposed as key intermediates in the catalytic nitrogen reduction cycle and characterise them. These intermediates where then subjected to the same catalytic conditions, resulting in comparable NH_3 yields. This verified such intermediates as part of the nitrogen reduction cycle, including [HIPTMo]N_2, [HIPTMo]N and others, and allowed the authors to achieve yield efficiencies of ~ 65%, normalised to the number of reducing equivalents; comparable to nitrogenase (figure 1 b-d) [19]. Since the initial success of Yandulov and Schrock, there have been several other attempts to achieve ambient ammonia

synthesis catalysed by transition metal complexes. Notably, the use of Mo-based complexes bearing pincer ligands by Nishibayashi and coworkers has proven highly successful[31,78–83].

[H2] Active centre

The interest in molybdenum based molecular complexes arose from the false premise that molybdenum in the FeMo-co of nitrogenase was critical for nitrogen reduction[34]. The discovery that the active site for nitrogen reduction is in fact the iron atoms led to a greater degree of interest in iron-based homogeneous catalysts. In 2013, Peters and co-workers showed that nitrogen reduction to ammonia was possible on a tris(phosphine)borane-supported iron complex ($P_3^BFe^+$)[84,85], as shown in figure 1 b-d. The Nishibayashi group also developed Fe based systems, with an Fe based complex bearing a pyrrole based PNP (PNP = 2,6-bis(di-tert-butyl-phosphinomethyl)pyridine) pincer ligand being shown to generate catalytic quantities of ammonia[86]. Several other homogeneous catalysts have been developed, which move away from the bio-inspired use of Mo or Fe as an active site. The Peters group established that the Co analogue (P_3^BCo) was capable of reducing nitrogen to make ammonia, which was the first demonstration of nitrogen reduction using a non-Mo or Fe based complex[34,87]. Nishibayashi and coworkers also developed other metal complexes with pyrrole based PNP pincer ligands. While the Nishibayashi Co based complex significantly outperformed its Fe based counterpart[86,88], the Peters Co based catalyst experienced a 2.9 fold decrease in yield compared to its Fe equivalent[87]. The Nishibayashi group also developed a V complex bearing pyrrole-based PNP pincer ligands, which produced a yield on the same order as the equivalent Co and Fe complexes[88]. The Peters group have also tested metal complexes with active sites such as Os and Ru, which have both been shown to be capable of reducing nitrogen[34,89]. It is interesting to note that only the Mo based complexes are able to efficiently produce ammonia at ambient temperature and pressure; catalysts based on other metals must operate at cryogenic temperatures[34,53]. This is a surprising result, given that it is unlikely that Mo plays a role in binding to nitrogen in the FeMo-co[37]. The required cryogenic operating temperature for other metallic centres is related to the stability of the reduction environment to hydrogen evolution as well as the thermal stability of key reaction intermediates. Indeed, Peters and co-workers have shown that the first N-H species formed on a transition metal complex have weak N-H bonds, leaving them vulnerable to deleterious hydrogen evolution over ammonia formation. Mo species have a stronger N-H bond, allowing them to operate at more moderate conditions and overpotentials than Fe based species[90].

[H2] Proton source

The controlled addition of protons and electrons, critical in nitrogenase, is also crucial for homogeneous catalysis. The transfer of a single proton to the catalytically active site in a single step via proton-coupled electron transfer (PCET), where protons and electrons are transferred together, or hydrogen atom transfer facilitates the formation of N-H bonds towards NH_3 formation[28]. However, Yandulov and Schrock noted that the stepwise accumulation of hydrogen atoms, but via separate protonation and reduction steps, at the active site was key to efficient nitrogen reduction, as shown in figure 4a[19,91]. In addition, [LutH][BAr^F_4] (Lut = 2,6-dimethylpyridine, BAr^F_4 = tetrakis[3,5-bis(trifluoromethyl)phenyl]borate) was chosen as a proton source in part due to the fact that it is a weak acid, having a pKa of 6.75 in water[92]. This means that it is a relatively poor proton donor[93].

Peters and coworkers first used a very strong acid, $[H(OEt_2)_2]^+B[(3,5\text{-}CF3)_2C_6H_3]^{4-}$ ($HBArF_4$, pK_a ~ 0 in THF), when testing their P_3BFe^+ catalyst and obtained a yield that was lower than contemporary Mo based catalysts, despite using a strong reducing agent, KC_8 (U = -2 V vs RHE (See supporting information))[85], and operating at -78°C to suppress hydrogen evolution[34,84]. However, by utilizing $[Ph_2NH_2][OTf]$ or $[PhNH_3][OTf]$ (pK_a in Et_2O relative to $(Et_2O)_2H^+$ 1.4 and 6.8 respectively) and CoCp*2 (U = -0.98 V vs RHE ($[Ph_2NH_2][OTf]$) or U = -0.76 V vs RHE ($[PhNH_3][OTf]$) (See supporting information)) they could reach a higher selectivity and catalytic turnover for NH_4^+ by allowing for a hydrogen atom transfer mechanism to occur. This reduced the high thermodynamic cost of protonating the ligated nitrogen atom, with steric hindrance protecting the reduced metal site from deleterious hydride formation[85]. Chalkley et al. were also able to show that the pK_a value of the proton source has a significant impact on the selectivity of the catalyst, with an intermediate pK_a value providing the most favourable percentage yield of ammonia for their P_3BFe^+ catalyst, as shown in figure 4 (b)[94]. Ashley and co-workers also noted a dependence of the efficiency of their catalyst, $Fe(N_2)(depe)_2$ (depe = $Et_2PCH_2CH_2PEt_2$), on the acidity of their proton donor, showing that a moderate level of acidity yielded the best result. Interestingly, this catalyst is the only homogeneous system capable of selectively reducing N_2 to N_2H_4[95,96].

Nishibayashi and co-workers report the remarkable effect of using a coordinating proton source and single-electron reducing agent, achieving markedly improved performance of the same catalyst by using SmI_2 (U = -1.9 vs RHE (see supporting information)) and ethylene glycol or water compared to their earlier reported use of $CoCp^*_2$ and [ColH]OTf [31,97]. This system was shown to have 91% selectivity towards ammonia, and has the highest turnover of any other homogeneous catalyst considered[31]. It even outperforms some solid electrodes in terms of stability (figure 1 b-d). When water coordinates with SmI_2 to form $[Sm(H_2O)_n]^{2+}$, it lowers its pK_a value. The O-H bond dissociation free energy in free water is 464.4 kJ mol^{-1}, whereas, upon coordination to SmI_2, it drops to around 133.9 kJ mol^{-1}, with a pK_a of around 3.3 in water[98]. This could push the pK_a to the more favourable region, as shown in figure 4b. However, more thorough theoretical studies are required to confirm this hypothesis as it depends on whether H^+ or hydrogen atom transfer is mechanistically required for the catalysts in question.

In addition, the size and solubility of the proton source was shown to affect selectivity. Mössbauer and EPR spectroscopy results considering the Peters P_3BFe^+ catalyst revealed that the protonation rate was slow when using $[Ph_2NH_2][OTf]$, the acid which afforded the best selectivity. When the proton source was replaced with a more soluble acid, $[Ph_2NH_2][BAr^F_4]$, the percentage yield decreased[85]. As for proton source size, research has shown that bulky acids can prevent the formation of metal hydrides and suppress competing hydrogen production. Examples of such bulky acids, $[LutH]^+$ or $[Ph_2NH_2]$ (2,2'- diphenylamine), have been shown to successfully limit the access of protons to the active metals. Arashiba et al. also observed a strong influence on the catalytic activity of Mo complexes bearing PNP ligands depending on the counter-anion of the lutidinium salts acting as proton sources. They observed that when utilizing tetraarylborate ($[LutH]BAr_4$, Ar = $3,5\text{-}(CF_3)_2C_6H_3$) or chloride ([LutH]Cl) the yield of ammonia dramatically decreased. Only by using triflate ([LutH]OTf, OTf = OSO_2CF_3) can the catalytic reduction of nitrogen be achieved. This was attributed to the lower coordination ability of OTf to Mo atoms and therefore a more feasible regeneration of

the dinitrogen complex under catalytic conditions[78]. Furthermore, an increased quantity of proton source also lowers the selectivity of the process[99].

All these findings echo the original results of Yandulov and Schrock[19], suggesting that controlled protonation is critical for increased selectivity, similar to the relationships seen in nitrogenase[43,44]. However, there is more information available regarding homogeneous catalysis, perhaps due to the increased ease with which the molecular species can be interrogated using a variety of spectroscopic techniques, and readily structurally elucidated using single-crystal X-ray diffraction. This is one of the key benefits of homogeneous catalysis.

[H2] Reaction pathways

The ability to interrogate molecular species also allows reaction pathways to be more easily elucidated across homogeneous catalysts. The Schrock cycle, shown in figures 4a and 2, occurs via the stepwise protonation and reduction of the bound dinitrogen at the molybdenum centre[19,100]. Here the dinitrogen triple bond is not broken until the first NH_3 molecule is released, making it an associative nitrogen reduction scheme. It is likely that the Peters P_3BFe^+ catalyst proceeds via a similar associative nitrogen reduction scheme due to the observation of a kinetically stabilised Fe-NNH diazenido species via EPR spectroscopy[90].

Molybdenum based catalysts bridged by dinitrogen bearing pincer ligands, such as the PNP or PCP ligands used by Nishibayashi and coworkers[31,79], follow different paths depending on the method of generating a molybdenum nitride intermediate complex[100]. For some complexes, protonation of the terminal dinitrogen not involved in bridging the complex results in ammonia generation. For others, it is more likely that the bridging dinitrogen itself is cleaved to afford two separate complexes, which then generate ammonia as per the scheme shown in figure 2[100]. It is likely that the dinitrogen bridged MoX_3(PNP) based catalysts pioneered by Nishibayashi and coworkers and (Figures 1 b-d) proceed via direct dinitrogen triple bond cleavage when using $CoCp^*_2$ and [ColH]OTf (combined U = -1.3 V vs RHE, see Supporting Information) as reductant and proton source respectively[97]. However, the dinitrogen bridged $MoCl_3$(PNP) based complex is likely to proceed via protonation of the terminal dinitrogen when using $CoCp_2$ and [LutH]Otf[78] (combined U = 0.91 V vs RHE, supplementary). It is likely that the $MoCl_3$(PCP) based dinitrogen bridged complex proceeds via direct dinitrogen cleavage when using a combination of SmI_2 and water as reductant and proton source[31]. Since dinitrogen cleavage is energetically expensive, it makes sense that those systems following the direct N_2 cleavage pathway require a stronger reducing agent and proton source combination. Indeed, Ashida et al. note a relatively high overpotential for their $MoCl_3$(PCP) based dinitrogen bridged complex using SmI_2 and water[31]. However, following the direct N_2 cleavage pathway usually results in increased ammonia yields[100].

While the Schrock cycle operates via the stepwise addition of protons or electrons[19], there is some evidence that some reactions may proceed at least partially by PCET. For the Nishibayashi catalyst operating using SmI_2 and ethylene glycol, there is evidence for at least the first N-H bond to form via PCET[100]. Chalkley and Peters note that the first N-H bond is likely to be the most energetically difficult of all protonation steps since it has a very low bond dissociation free energy[90]. Chalkley et al. also note that using milder reducing agents and proton sources can allow for higher effective bond dissociation energies, which in turn makes PCET more favourable[85]. In general, PCET is a less energy intensive process than the stepwise

addition of protons and electrons observed by Yandulov and Schrock[19,100]. Further studies are required to elucidate exactly which method of proton and electron transfer to the active site is the most favourable for nitrogen reduction.

[H2] Steric protection

The performance of a nitrogen reduction catalyst is highly dependent on its coordination sphere. The steric bulk of the ligands can determine the nature of the N_2 coordination to the metallic moieties (end-on or side-on)[101] and electronic effects can alter the catalytic activity of the complex[1]. Utilizing bulky ligands is desirable to protect the active centre against poisoning from hydrogen as well as for stabilization of the reaction intermediates[102]. Weare et al. observed that, upon protonation of a Mo-dinitrogen complex with trisamidoamine ligands via proton coupled electron transfer, dihydrogen was formed in the absence of a sufficiently sterically bulky ligand[103]. Phosphine-based pincer ligands are some of the most utilized due to their steric bulk, molecular versatility, and possibility of conforming supramolecular assemblies via hydrogen bonding[104]. These supramolecular assemblies can be used for tailoring the molecular complex distortion, similar to the dynamic structure of nitrogenase, which can alter the selectivity of the complex to nitrogen reduction[105]. Previous studies based on hydrogen evolution catalysts focussed on the effect of changing phosphine substituents, and confirmed that more bulky substituents on phosphorus atoms result in larger tetrahedral distortions and a higher hydride affinity[106,107]. Nishibayashi and coworkers confirmed the favourable effect of PNP ligands in the catalytic activity of Mo-N_2 complexes versus strongly-binding monodentate ligands [31,108]. The electronic versatility of the ligands is also relevant, owing to the stabilization of different oxidation states of the active centre during catalysis. In addition, strong donor groups such as carbenes[109], amides[92] or phosphines are necessary to induce pi-back-bonding to the N_2 from the metal, promoting its activation. The steric bulk of PNP pincer ligands has also been shown to stabilize the singlet ground state through a robust N → metal π-donation due to the square-planar coordination geometry, while the utilization of disilylamido ligands results in an intermediate spin ground state owing to a weaker π-donation[110].

The stability of the catalyst induced by the coordination sphere determines the overall performance; strong donor ligands which afford robust metal-ligand bonds improve the stability as well as increasing selectivity by steric protection, although most turnover numbers are often still low in comparison to the lithium mediated system or nitrogenase (figure 1d).

[H1] Challenges in aqueous electrolytes

Considering the wealth of knowledge available in aqueous electrochemistry, it would be convenient to carry out nitrogen reduction over a solid electrode in an aqueous electrolyte. However, there are substantial roadblocks to this goal. Recent work highlights the similarities between problems faced in CO_2 and N_2 reduction in aqueous electrolytes, namely the competition with the hydrogen evolution reaction and operation at a high overpotential[111]. Interestingly, nitrogenase can reduce both CO_2 and N_2, highlighting nitrogenase's unique ability to circumvent hydrogen evolution and the potential similarity between the two reduction reactions. A prerequisite for both CO_2 and N_2 reduction catalysts are a catalyst which preferentially adsorbs the molecule of interest (*CO for products beyond $CO_{(g)}$ from CO_2 and $*N_2$ for ammonia production, respectively) over *H to enable a reduction reaction to compete with hydrogen evolution in aqueous media[111].

[H2] Scaling relations

*H coverage is a significant problem faced by catalysts for both CO_2 and N_2 reduction[46,47], shown schematically in figure 5a. For nitrogen reduction catalysts, this occurs as a result of unfavourable scaling between $*N_2$ and *H binding energies, also meaning that typical selectivities towards ammonia in aqueous electrolytes are negligible[11,112]. Indeed, catalysts able to bind N_2, including the catalytic cofactors of the three nitrogenase variants, under ambient conditions in aqueous electrolytes will always preferentially adsorb hydrogen[111], as shown in figure 5b. In this plot, catalysts below the horizontal line have favourable N_2 adsorption thermodynamics, and those to the right of the vertical line do not bind strongly to *H. Pristine nitrogenase is exactly at the vertical line and so does not preferentially bind $*N_2$. Thus, pristine nitrogenase behaves as hydrogenase, whereas removing the bridging sulfur allows for an activated nitrogenase which can bind and catalyse $*N_2$. Notably, catalysts below the horizontal line are also in the lower left quadrant, meaning that they also bind strongly to *H and function as HER catalysts[111].

A second scaling relation must also be considered which also affects catalysts able to circumvent the hydrogen evolution problem. Figure 5c shows potential reaction pathways for the associative nitrogen reduction mechanism, believed to be the most likely mechanism under ambient conditions, across Au(211) and Re(111), where the ideal catalyst is one that remains as close as possible to zero change in free energy. Both pathways encounter relatively severe uphill reaction steps, a problem which nitrogenase avoids (figure 3 d-f) and allows it to operate at a mild overpotential. From these free energy diagrams, the limiting potential, U_L, can be obtained, defined as the minimum potential required to make every step in the mechanism downhill in energy[113]. Here, the scaling relation between key nitrogen reduction intermediates, specifically $*N_2H$ and *NH, severely limits the energy efficiency of electrochemical ammonia synthesis, as shown in figure 5d. This scaling fixes the minimum limiting potential for ammonia synthesis via the associative pathway at approximately - 0.5 V vs RHE[113], similar to the limiting potential for nitrogenase (approximately -0.8 V vs RHE, suggesting that it is likely to follow an associative reduction pathway)[114]. Such a limit on potential efficiency is problematic for ammonia for use as a fuel[9]. In this case, a catalyst which reduces nitrogen along the dissociative pathway, such as lithium, may provide a better solution. However, here the potential limiting step is Li^+ reduction which fixes the potential at even more negative values (figure 1 b-d).

[H3] Is there a material that can circumvent HER and break scaling relations?

Given the limitations imposed on overpotential and selectivity by scaling relations between nitrogen reduction intermediates and hydrogen, there has been a considerable amount of interest in finding a new electrocatalyst which can improve scaling relations. In particular, theoretical calculations have suggested that early transition metals[47], transition metal nitrides [115–120] and dual atom catalysts[121,122] could work as nitrogen reduction reaction catalysts at ambient conditions.

Transition metal electro-catalysts were studied for N_2 reduction through Density Functional Theory (DFT) calculations, simulating both the associative and dissociative mechanisms by Nørskov and co-workers. Though the mid to late transition metals such as Mo, Fe, Rh and Ru exhibit the most optimal binding to nitrogen, they have a high affinity for hydrogen atoms

which lowers their Faradaic efficiency towards NH_3 production. Early transition metals, such as Sc, Y, Ti or Zr, however, were suggested to exhibit higher selectivity towards N-adsorbates and could therefore produce higher ammonia quantities at an applied bias between –1.0 and -1.5 V vs SHE via the dissociative mechanism, as highlighted in figure 2[47].

Transition metal nitrides were studied theoretically by Skulason and coworkers, who highlighted that nitrogen reduction could proceed via a Mars-van Krevelen mechanism, where lattice nitrogen atoms are protonated to ammonia, as shown in figure 2. Once this ammonia molecule has been released, the resulting nitrogen vacancy is filled by a new nitrogen atom, which can then also be protonated to ammonia and complete the cycle. This mechanism improves the scaling between adsorbates and requires a much lower overpotential for nitrogen reduction than conventional associative or dissociative mechanisms[116]. Indeed, N_2 adsorption and subsequent reduction to $*N_2H$ is strongly facilitated relative to *H adsorption by at least 1 V, according to DFT calculations[47].

Moving away from a continuous distribution of active sites, dual atom catalysts, surrounded by electron donor heteroatoms, have been theorised as promising candidates for nitrogen reduction[121]. Such systems mimic nitrogenase, and could result in decreased overpotential and dissociation barriers for N_2 [122]. Nørskov and co-workers showed that isolated metal atoms, such as Re dimer single atoms within Cu (211), forced a singly coordinated dissociative adsorption of N atoms, breaking the transition-state scaling relation[122]. The removal and return of H_2S groups in nitrogenase which allows the enzyme to break free from unfavourable scaling between H* and N* binding energies (figure 3d-f)[37] which could be emulated using dual atom catalysts through potential modulation.

However, despite promising theoretical motivation[123–125], the practical employment of the these three paradigms in aqueous electrolytes have been unsuccessful. Any putative reports of N_2 reduction on transition metal nitride surfaces have later been debunked[126,127]. The key reason for this discrepancy may be that the theoretically predicted nitride surfaces are highly challenging, if not impossible, to realise experimentally. Transition metal nitrides are unstable towards bulk oxide formation[128]. Once a 3D oxide has been formed, it is likely to be poorly conducting and difficult to remove. X-ray photoelectron spectroscopy (XPS) measurements showed that a freshly deposited MoN film prepared by reactive sputtering had a significant surface oxygen content of 28%, which increased to 50% after a week of air exposure[128]. Since XPS is a highly surface sensitive technique, this is likely to mean that the surface is a pure oxide. X-ray Diffraction (XRD) and XPS data from Simonov and coworkers also reveals the presence of oxide species in their VN and NbN films, which they were unable to remove[127]. Studies on the suitability of early transition metal nitrides for the oxygen reduction reaction show that transition metal nitrides bind too strongly to oxygen, resulting in a lack of oxygen dissociation[129]. Pure early transition metals suffer from the same strong binding to oxygen[130]. For dual atom catalysts, the isolated metal sites upon which they depend have a significant driving force to be reduced and agglomerated into clusters or nanoparticles under reducing conditions[124]. Mougel and co-workers observed that Cu single atoms supported in an N-doped carbon material were reduced to Cu nanoparticles upon application of a cathodic voltage under CO_2 reduction conditions[131]. Other metal dopants are more stable. For instance, Gu et al. observed that Fe^{3+} single atoms with pyrrolic coordination were stable at potentials positive of -0.5 V vs RHE; at more negative potentials they reduced to Fe^{2+}[132].

[H2] The end for aqueous nitrogen reduction?

Nitrogen reduction is therefore exceptionally challenging to catalyse in ambient conditions. In aqueous media, deleterious competition with the HER causes electrode poisoning and deactivation[47], with negligible selectivities [112] and the literature is saturated with false reports due to contamination, as previously discussed[16,20,112,133]. The catalytic reaction is hindered by fundamental scaling between intermediates, forcing the overpotential to unfavourable regions[113]. Promising catalysts revealed by DFT prove extremely difficult to realise under experimental conditions[126–128], and other reports fail to rigorously account for background contamination sources, rendering the results inconclusive[14,20]. The requirement of a highly reactive catalyst to break the dinitrogen triple bond[134] causes experimental difficulties since the highly reactive surfaces are unstable, likely to form oxides and suffer from active site poisoning. If it were not for the existence of nitrogenase, efficient N_2 reduction would seem impossible under ambient conditions.

[H1] Translating insight across fields

A solution to the problem of aqueous electrolytes for solid electrodes could be found by lowering the chemical potential of water or protons, which may destabilise the binding of H*[111]. This would suppress the HER and promote nitrogen reduction, as shown in figure 5b, allowing promising catalysts such as Ru or Fe to function with improved efficiency[111]. This is analogous to nitrogenase and homogeneous catalysis, where greater selectivity towards nitrogen reduction can be achieved by restricting the access of protons to the catalytic active site.

[H2] Microkinetic modelling

The microkinetic model of Singh et al. reveals that the rate equations for nitrogen and hydrogen adsorption at the potential required for nitrogen reduction can be written as

$$r_N = k_N \theta_N \widetilde{c_+}\widetilde{c_-} \longrightarrow k_N \frac{K_N}{K_H} \widetilde{c_{N_2}}, \qquad 2$$

$$r_H = k_H \theta_H \widetilde{c_+}\widetilde{c_-} \longrightarrow k_H \widetilde{c_+}\widetilde{c_-}, \qquad 3$$

where K_N and K_H are the equilibrium constants for associative nitrogen and hydrogen adsorption, respectively. The concentrations of protons, electrons and dinitrogen near the electrode surface are written $\widetilde{c_+}$, $\widetilde{c_-}$ and $\widetilde{c_{N_2}}$, and k_N and k_H are the respective forward rate constants[11]. Therefore, selectivity towards nitrogen reduction is negligible in aqueous electrolytes due to the increased proton activity. However, at high overpotentials on strongly binding catalysts, tuning the proton concentration can lead to sizable changes in selectivity. At high overpotentials the system is governed by surface coverage, which, as shown in equations 2 and 3, is first order in proton concentration for hydrogen adsorption but zeroth order in proton concentration for nitrogen adsorption. Therefore, Singh et al proposed the three necessary reaction conditions for a *selective* catalyst are (i)a strongly binding catalyst, (ii) a large overpotential and (iii) a non-aqueous electrolyte with reduced proton activity[134]. However, we emphasise that, while reducing the proton concentration will increase *selectivity*, decreasing it may come at the cost of *activity*. If you had an ultra-selective

electrochemical device but with very little activity, it would be prohibitively expensive to produce any ammonia. A moderate proton concentration at the electrochemical interface would allow for a balance of improved selectivity and reasonable activity[135].

[H2] Lithium-mediated nitrogen reduction

The only electrochemical system to date that has been rigorously verified as an ammonia producer is that pioneered by Tsuneto et al. in their 1993 and 1994 papers[20,22,23], shown schematically in figure 6. The secret to the success of this system could be the restriction of protons to the electrode surface by the growth of a passivating layer, known as the Solid Electrolyte Interphase (SEI). Indeed, a common thread between successful biological and homogeneous catalytic systems for nitrogen reduction is the restriction of access of protons to the catalytically active site. As discussed in the previous section, steric protection of the active site in homogeneous systems leads to better catalyst performance[19,78], as does the use of weak, bulky proton donors[19]. The FeMo-co utilises sulfur atoms to provide a degree of steric protection to the active site[37,136]. It is also clear that the hydrophobic and anhydrous environment surrounding the FeMo-co and controlled protonation via a proton wire is key to nitrogenase's selectivity[43,44].

In the lithium mediated system, the electrolyte is made up of an organic solvent, a proton source and a lithium salt[20,22,23,29,30,137–143]. Tsuneto et al. noted that the choice of electrode material resulted in differing activity towards nitrogen reduction, evaluating mechanically polished polycrystalline metal samples such as Ti, Ag and Mo, stating that this was due to how readily the electrode metal forms an alloy with lithium and emphasising the necessity for the availability of fresh lithium[23]. In Tsuneto et al's experiments the electrode material served as a current collector, which may influence the morphology of the lithium containing deposits formed in situ, but the N_2 fixation itself would occur on the lithium surface. The mechanical polishing and air transfer that Tsuneto et al would have employed on surfaces such as Fe or Ti would result in the formation of passivating oxides (see Section 4a), which would not have reduced under reaction conditions. The in-situ deposited lithium would not be covered by native oxides, which could explain its greater reactivity towards N_2.

The fact that lithium metal has the ability to spontaneously split the highly stable dinitrogen bond at ambient temperature and pressure, which can be rate limiting in other systems[139], certainly aids the reaction. However, there are other metals which can dissociate dinitrogen in the same way, such as early transition metals[47]. It is also important to note from Figure 5b that Li containing electrodes including Li_3N, LiN_3, and Li, hypothesised as the active surface for lithium mediated nitrogen reduction by Schwalbe et al.[142], bind *H much more strongly than they bind $*N_2$. These surfaces will therefore intrinsically favour H_2 evolution[111]. Still, Tsuneto et al.'s work implies that the presence of a lithium salt is critical for efficient ammonia synthesis, as well as the availability of fresh lithium[22,23]. Hence understanding the unique ability of lithium to drive N_2 electrochemical reduction requires us to go beyond merely considering the properties of the electrode[135]. The uniqueness of the lithium could lie in its properties as a solvated cation, as observed in battery science.

The energy output of a Lithium-Ion Battery (LIB) is defined by its open-circuit voltage, which is equal to the difference between the electrochemical potentials of the anode and cathode. In order to avoid runaway electrolyte decomposition, which would compromise battery

stability, this voltage must lie within the voltage window of the electrolyte, which is defined as the difference between the Highest Occupied Molecular Orbital (HOMO) and Lowest Unoccupied Molecular Orbital (LUMO) of the electrolyte[144–146]. However, most anodes and cathodes used in LIBs are highly reactive, meaning that these requirements for thermodynamic stability are not met. Yet, battery systems achieve kinetic stability through the growth of a passivating layer on the electrode surface, known as the Solid-Electrolyte Interphase (SEI)[147], first observed in 1979 by E. Peled[148]. The SEI consists of an inorganic layer close to the electrode surface and a thicker polymeric layer at the interface with the electrolyte[149–151]. This SEI is formed from the decomposition products of the organic electrolyte and lithium salt and is dependent on the electrode work function; Ir(111) electrodes catalyse SEI formation at much lower overpotentials than Cu(111)[152]. In particular, lithium cations are the most effective at forming the SEI, because of their high Lewis acidity enabling the efficient abstraction of protons through a strong affinity to proton donor anions[153]. SEI stability is critical to LIB performance; if the SEI cracks or dissolves, runaway electrolyte decomposition will occur, limiting battery lifetime[151]. SEI aging and continued growth, particularly via deposition of degradation products from the cathode, can also increase electrode impedance and loss of lithium inventory[154]. Ideally, the SEI should be homogeneous, thin, electrically insulating but conductive to Li^+ ions and mechanically strong in order to ensure its stability[155].

Since the lithium mediated nitrogen reduction system in question employs an organic electrolyte and lithium salt, an SEI will form[30,142]. The SEI could restrict the access of protons to the surface of the electrode, limiting the problem of electrode poisoning in aqueous electrolytes[11,47,113,134], and mimic the anhydrous, aprotic environment which allows for the success of the nitrogenase enzyme[43]. Krishnamurty et al.'s work using a machine learning approach to examine potential proton donors for lithium mediated nitrogen reduction found that proton donors with intermediate pKa perform best[156]. This is in analogy to the dependence of activity on pKa for nitrogenase and homogeneous catalysts, as shown in figure 4b. Tsuneto et al. investigated the effect of using a different salt cation in their system, noting that the use of Na^+ or Bu_4N^+ resulted in a negligible ammonia yield[23]. The burgeoning field of sodium ion battery research is hampered by the lack of a functioning SEI; the sodium based SEI components are far more soluble than their lithium based counterparts[157]. The presence of fluorine could also be useful. In electrolytes containing HF contaminants, this has been shown to aid the formation of a layer of LiF which passivates the electrode surface and inhibits hydrogen evolution[152,158], which could be aiding the efficiency of electrolytes containing $LiBF_4$[29,139–141]. It is also interesting to note that recent work by Li et al. has shown improved stability and efficiency by including small quantities of O_2 in their inlet gas stream, while bulk amounts decrease faradaic efficiency[137]. This is a counterintuitive result, given that any O_2 inclusion results in catastrophic efficiency loss for nitrogenase[68]. The authors attribute this improved efficiency and stability to the influence of the oxygen on SEI homogeneity, reduced Li^+ diffusivity and content, with an increase in inorganic species such as Li_2O as evidenced by XRD. The reduction in Li^+ diffusivity would result in fewer electrons being used up in Li plating rather than in nitrogen reduction, increasing the faradaic efficiency. The increased SEI homogeneity and inorganic content would result in a more stable, less electronically resistive SEI[137].

To fully understand the impact of the SEI on nitrogen reduction, a thorough characterisation of the SEI components is required. However, SEI characterisation is notoriously difficult. Not only are SEI components highly air and water sensitive[149], making it difficult to transport samples to ex-situ characterisation equipment, but many ex-situ characterisation techniques require washing stages during sample preparation which can remove weakly bound species. For example, a comparison of in-situ neutron reflectometry and ex-situ X-ray Photoelectron Spectroscopy (XPS) data reveals discrepancies likely due to the removal of SEI components during XPS sample preparation[159]. Some in-situ techniques, such as Electrochemical Atomic Force Microscopy (EC-AFM)[155], operando Fourier Transform Infrared (FTIR) spectorscopy[160] and Raman spectroscopy[161] have been successful in battery systems. A particularly useful side effect of SEI formation is gas evolution, which can be used to identify SEI components and formation mechanisms. To the authors' knowledge, there has been little attempt in the literature to carefully characterise the SEI layer formed during lithium mediated nitrogen reduction or a full investigation into its effect on ammonia synthesis. Indeed, the properties of an ideal SEI for nitrogen reduction might differ significantly from those in Li ion batteries (which have been more extensively characterised), in part due to the desire to limit Li^+ diffusivity for the former[137] and enhance it for the latter. Thus, though much can be learned from the battery community, a new thinking for Li SEIs might be required for nitrogen reduction.

While there has been a great amount of interest in the lithium mediated system, the exact mechanism by which dinitrogen is reduced to ammonia is still disputed. In the original work of Tsuneto et al., the authors suggested that fresh Li metal is required to split the highly energetic nitrogen triple bond, and the resulting Li nitride is then further protonated to ammonia by the proton donor, ethanol[22,23]. Lazouski et al. later proposed a microkinetic model to explain transport limitation effects in the system[139] and developed a non-aqueous gas diffusion electrode method to overcome this[29]. Chorkendorff and coworkers. have proposed a simple molecular model for ammonia synthesis in the lithium mediated system, proposing that balancing the concentrations of nitrogen and hydrogen relative to that of the lithium metal can lead to improved faradaic efficiencies[30], which is further expanded upon in their more recent work[137]. Schwalbe et al. proposed a heterogeneous mechanism for nitrogen reduction across a surface made up of a combination of lithium, lithium nitride, lithium hydride and other mixed species[142]. A schematic of the current understanding of the system is shown in figure 6. However, the exact electrochemically active surface is unknown.

Although the lithium mediated system has shown great promise, there are several drawbacks. Relying on fresh lithium electrodeposited in-situ requires operating at lithium plating potentials, which builds in a large intrinsic overpotential. This results in very low energy efficiences[29,30,137], further hindered by the highly resistive electrolyte[29]. There is also a well-documented problem with working electrode instability when using the Tsuneto electrolyte, where the potential drifts to more negative potentials with time. This limits the operating time of the system to a few hours under constant chronopotentiometry[22,30]. The use of a sacrificial proton donor is also problematic[30,140], and only low current densities of under -10 mA cm^{-2} are generally possible[20,30,139]. Various optimisation strategies are highlighted in figure 1(b-d). Andersen et al. devised a cycling method to improve stability[30], and Suryanto et al. used a recyclable proton donor which improved efficiency and stability, as well addressing the problem of a sacrificial proton donor. However, it must be noted that the basic

environment used by Suryanto et al. results in an even more negative operating potential vs RHE[140]. Krishnamurthy et al. devised a machine learning framework to speed-up the discovery of other promising proton donors, showing that ethanol's intermediate pKa could be the reason for its success in lithium mediated nitrogen reduction[156], and Lazouski et al recently provided an updated model to describe the effect on Faradaic efficiency of differential transport created by different proton donors[162]. Lazouski et al. have also investigated the issue of transport limitation by designing a novel gas diffusion electrode[29]. Li et al have increased the achievable current density through the use of a high surface area Cu electrode, achieving high ammonia production rates of 46.0 ± 6.8 nmol s^{-1} cm_{geo}^{-2}, but only moderate faradaic efficiencies of 13.3 ± 2.0 % at 20 bar N_2[138]. The same authors also used O_2 inclusion to achieve improved stability and efficiency, reaching 78 ± 1.3 % at 20 bar N_2[137]. Recently, Du et al were able to achieve close to 100% Faradaic efficiency and stable operation by utilising a new salt, $LiNTf_2$, nickel wire electrode and operating at higher salt concentrations under 15 bar N_2[141]. Despite these breakthroughs, figure 1(b-d) still shows that there is still a long way to go before the system is economically viable in comparison to the well optimised Haber Bosch process[25]. Indeed, even if there were no Ohmic or transport losses and 100% Faradaic efficiency, the maximum possible energy efficiency would still be low. Considering the lithium mediated system, which generally operates at -2.7 V vs RHE with an anodic potential of approximately +0 V vs RHE, and couple this to water oxidation, with a thermodynamic potential of 1.2 V, this would limit the maximum thermodynamic energy efficiency to 30% [139]. Therefore, its reliance on in-situ plated lithium greatly sets a hard limit to the maximum energy efficiency of the lithium mediated system.

[H2] Reactant availability

While the lithium mediated approach in organic electrolytes has received recent attention, there are other methods of reducing the proton activity to promote selectivity towards nitrogen reduction. One example is avoiding competition between the N_2 reduction and hydrogen evolution reaction altogether by using a cycling method[163–165]. In general, the access of reactants to the catalytic centre in different systems determines the overall activity towards the formation of ammonia. Table 1 shows how the access of reactants to the catalytic surface affects selectivity and activity towards ammonia for three rigorously verified systems.

[H1] Conclusions

All approaches to nitrogen reduction considered in this review highlight that the control of the access of protons (and potentially electrons) to the active site is key to selectivity. Nitrogenase exemplifies this through its reliance on a protective environment to be able to reduce nitrogen rather than evolve hydrogen[44]. This theme is further built upon when considering homogeneous catalysis, with the existence of an optimum pKa value for the protic additive[94] and the requirement for a sufficiently bulky[78] and moderately soluble[85] acid. For solid electrodes, it is unlikely that electrocatalytic nitrogen reduction is possible in aqueous electrolytes at all due to extreme competition with hydrogen evolution[19,47,113]. However, by reducing the access to protons at the electrochemical interface, higher selectivities can be achieved[11,134], although there may be a payoff between selectivity and activity[135]. The challenges of N_2 fixation aqueous electrolytes has led to a greater interest in non-aqueous systems, in particular using a lithium mediated system[20,29,135,139–142].

While bioinspired systems such as the molecular complexes designed by the Peters[34,84,85,89,94,166] and Nishibayashi[31,78,81,82,97,167–170] groups have achieved high yields and faradaic efficiencies, their systems suffer from low turnover numbers. The Peters P_3^BFe and P_3^BCo catalysts were only able to complete around 13 and 2 turnovers respectively[34], and one of the Nishibayashi Mo based catalysts produced ~92% of its total yield within the first 30 minutes of an 18 hour long experiment[31]. The initial Schrock catalyst could only sustain 6 catalytic turnovers before deactivation[19]. This lack of stability limits the applicability of such systems for large scale ammonia production. In addition, while nitrogenase functions effectively in biological systems, and there have been successful attempts to immobilise the MoFe protein on an electrode for bioelectrocatalysis[171], its size reduces its capacity for industrial scale ammonia synthesis (Figure 1a). The most viable option to provide a distributed, carbon free method of ammonia synthesis is therefore electrocatalytic nitrogen reduction over a solid electrode. However, there is still much to be learned about the lithium mediated system. While there exists a wealth of characterisation literature for the SEI layer in LIBs, the SEI is yet to be satisfactorily characterised within the nitrogen reduction paradigm and may prove to have different requirements to that of LIBs. Given the knowledge from homogeneous and biological systems, it is likely that this SEI plays a key role in imbuing the system with a moderate proton activity to promote nitrogen reduction over hydrogen evolution. It is critical, therefore, that this SEI be characterised in the existing system, as well as considering insight from battery science to direct research towards beneficial SEI layer design. There is also much to learn about the active surface for nitrogen reduction in the lithium mediated system, as well as the mechanism by which the N_2 reduction proceeds[139,142]. Hopefully, once our community has established the exact characteristics that enable the lithium-mediated system to be so unique, the field can move away from the use of fresh electroplated lithium and the hard limit on energy efficiency. Indeed, taking on board the lack of required immediate dissociation in nitrogenase or homogeneous electrocatalysis (see figure 2 and associated discussion) [37,111,114], it appears unlikely that immediate N_2 scission, and therefore the requirement of metallic lithium as an electrocatalyst, is a prerequisite for nitrogen reduction across a solid electrode. Instead, controlled protonation appears to be a greater driving factor for selectivity.

All new research must take place with careful consideration of the danger of adventitious contamination, with greater emphasis being placed on benchmarking background levels of ammonia and compulsory isotopic labelling experiments[15]. Care must also be taken to ensure the purity of the isotopically labelled inlet gas, since it often has a higher level of contamination[21]. Any papers proposing previously un-verified methods from any discipline that do not rigorously consider contamination must be discredited.

The interplay between these three systems (nitrogenase, homogeneous catalysis and solid electrode electrocatalysis) suggests that there is much to be gained from interdisciplinary communication. The success of non-aqueous electrolytes in solid electrode electrocatalysis could provide useful insight for homogeneous systems when considering the choice of proton donor. Moreover, insight into the factors controlling catalytic trends on solid electrodes could both explain the role of the reactivity of the transition metal centre in homogenous catalysts and enzymes. Similarly, learning how to tailor proton transport through the SEI in the lithium mediated system could inform us on the role of the anhydrous matrix in in nitrogenase. This review aims to highlight the key research themes across the three paradigms which will lead

to the greatest impact in understanding the fundamentals of nitrogen fixation across homogeneous catalysis, nitrogenase and solid electrode electrocatalysis.

We anticipate that scientific progress will lead to the discovery of other active materials beyond lithium, thereby increasing the energetic viability of electrochemical nitrogen reduction, breaking one of the most important bottlenecks in our transition to a net zero society.

[H1] References

1. van der Ham, C. J. M., Koper, M. T. M. & Hetterscheid, D. G. H. Challenges in reduction of dinitrogen by proton and electron transfer. *Chemical Society Reviews* **43**, 5183–5191 (2014).
2. Rapson, T. D. *et al.* Insights into Nitrogenase Bioelectrocatalysis for Green Ammonia Production. *Chemsu* **13**, 4856–4865 (2020).
3. Rivera Ortiz, J. M. & Burris, R. H. Interactions among substrates and inhibitors of nitrogenase. *Journal of Bacteriology* **123**, 537–545 (1975).
4. MacFarlane, D. R. *et al.* A Roadmap to the Ammonia Economy. *Joule* 1–20 (2020) doi:10.1016/j.joule.2020.04.004.
5. Seh, Z. W. *et al.* Combining theory and experiment in electrocatalysis: Insights into materials design. *Science (1979)* **355**, (2017).
6. Guo, W., Zhang, K., Liang, Z., Zou, R. & Xu, Q. Electrochemical nitrogen fixation and utilization: Theories, advanced catalyst materials and system design. *Chemical Society Reviews* **48**, 5658–5716 (2019).
7. Capdevila-Cortada, M. Electrifying the Haber–Bosch. *Nature Catalysis* **2**, 1055 (2019).
8. Gallucci, M. The ammonia solution: Ammonia engines and fuel cells in cargo ships could slash their carbon emissions. *IEEE Spectrum* **58**, 44–50 (2021).
9. Stephens, I. E. L. & Nilsson, A. Research needs towards sustainable production of fuels and chemicals, Section 5: Sustainable N2 reduction. *Energy-X* 49–57 (2019).
10. McPherson, I. J., Sudmeier, T., Fellowes, J. & Tsang, S. C. E. Materials for electrochemical ammonia synthesis. *Dalton Transactions* **48**, 1562–1568 (2019).
11. Singh, A. R. *et al.* Electrochemical Ammonia Synthesis—The Selectivity Challenge. *ACS Catalysis* **7**, 706–709 (2017).
12. Nørskov, J. K. *et al. Research needs towards sustainable production of fuels and chemicals*. *Energy-X* (2019) doi:10.4324/9780429047237-18.
13. Kibsgaard, J., Nørskov, J. K. & Chorkendorff, I. The Difficulty of Proving Electrochemical Ammonia Synthesis. *ACS Energy Letters* **4**, 2986–2988 (2019).
14. Choi, J. *et al.* Identification and elimination of false positives in electrochemical nitrogen reduction studies. *Nature Communications* 1–10 (2020) doi:10.1038/s41467-020-19130-z.
15. Iriawan, H. *et al.* Methods for nitrogen activation by reduction and oxidation. *Nature Reviews Methods Primers* **1**, 56 (2021).
16. Licht, S. *et al.* Retraction. *Science (1979)* **369**, (2020).
17. Field, L. D., Hazari, N. & Li, H. L. Nitrogen Fixation Revisited on Iron(0) Dinitrogen Phosphine Complexes. *Inorganic Chemistry* **54**, 4768–4776 (2015).
18. Mackellar, D. *et al.* Streptomyces thermoautotrophicus does not fix nitrogen. *Scientific Reports* **6**, 1–12 (2016).

19. Yandulov, D. V. & Schrock, R. R. Catalytic Reduction of Dinitrogen to Ammonia at a Single Molybdenum Centre. *Science (1979)* **301**, 76–79 (2003).
20. Andersen, S. Z. *et al.* A rigorous electrochemical ammonia synthesis protocol with quantitative isotope measurements. *Nature* **570**, 504–508 (2019).
21. Dabundo, R. *et al.* The contamination of commercial15N2 gas stocks with15N-labeled nitrate and ammonium and consequences for nitrogen fixation measurements. *PLoS ONE* **9**, (2014).
22. Tsuneto, A., Kudo, A. & Sakata, T. Efficient Electrochemical Reduction of N 2 to NH 3 Catalyzed by Lithium . *Chemistry Letters* **22**, 851–854 (1993).
23. Tsuneto, A., Kudo, A. & Sakata, T. Lithium-mediated electrochemical reduction of high pressure N2 to NH3. *Journal of Electroanalytical Chemistry* **367**, 183–188 (1994).
24. Nørskov, J. K. *et al.* Origin of the overpotential for oxygen reduction at a fuel-cell cathode. *Journal of Physical Chemistry B* **108**, 17886–17892 (2004).
25. Fourmond, V. & Léger, C. Dinitrogen Reduction: Interfacing the Enzyme Nitrogenase with Electrodes. *Angewandte Chemie International Edition* **56**, 4388–4390 (2017).
26. Rutledge, H. L. & Tezcan, F. A. Electron Transfer in Nitrogenase. *Chemical Reviews* **120**, 5158–5193 (2020).
27. Duval, S. *et al.* Electron transfer precedes ATP hydrolysis during nitrogenase catalysis. *Proc Natl Acad Sci U S A* **110**, 16414–16419 (2013).
28. Hoffman, B. M., Lukoyanov, D., Yang, Z. Y., Dean, D. R. & Seefeldt, L. C. Mechanism of nitrogen fixation by nitrogenase: The next stage. *Chemical Reviews* **114**, 4041–4062 (2014).
29. Lazouski, N., Chung, M., Williams, K., Gala, M. L. & Manthiram, K. Non-aqueous gas diffusion electrodes for rapid ammonia synthesis from nitrogen and water-splitting-derived hydrogen. *Nature Catalysis* **3**, 463–469 (2020).
30. Andersen, S. Z. *et al.* Increasing stability, efficiency, and fundamental understanding of lithium-mediated electrochemical nitrogen reduction. *Energy & Environmental Science* (2020) doi:10.1039/d0ee02246b.
31. Ashida, Y., Arashiba, K., Nakajima, K. & Nishibayashi, Y. Molybdenum-catalysed ammonia production with samarium diiodide and alcohols or water. *Nature* **568**, 536–540 (2019).
32. Jackson, M. N. & Surendranath, Y. Molecular Control of Heterogeneous Electrocatalysis through Graphite Conjugation. *Accounts of Chemical Research* **52**, 3432–3441 (2019).
33. Jackson, M. N., J. Kaminsky, C., Oh, S., F. Melville, J. & Surendranath, Y. Graphite Conjugation Eliminates Redox Intermediates in Molecular Electrocatalysis. *J Am Chem Soc* **141**, 14160–14167 (2019).
34. Chalkley, M. J., Drover, M. W. & Peters, J. C. Catalytic N 2 -to-NH 3 (or -N 2 H 4) Conversion by Well-Defined Molecular Coordination Complexes. *Chemical Reviews* **120**, 5582–5636 (2020).
35. Koper, M. T. M. & Heering, H. A. Comparison of Electrocatalysis and Bioelectrocatalysis of Hydrogen and Oxygen Redox Reactions. in *Fuel Cell Science: Theory, Fundamentals and Biocatalysis* 71–110 (2010).
36. Einsle, O. & Rees, D. C. Structural Enzymology of Nitrogenase Enzymes. *Chemical Reviews* **120**, 4969–5004 (2020).

37. Bukas, V. J. & Nørskov, J. K. A Molecular-Level Mechanism of the Biological N2 Fixation A molecular-level mechanism of the biological N 2 fixation. ***Preprint*** (2019) doi:10.26434/chemrxiv.10029224.v1.
38. Nørskov, J. K., Bligaard, T., Rossmeisl, J. & Christensen, C. H. Towards the computational design of solid catalysts. *Nature Chemistry* **1**, 37–46 (2009).
39. Pfisterer, J. H. K., Liang, Y., Schneider, O. & Bandarenka, A. S. Direct instrumental identification of catalytically active surface sites. *Nature Publishing Group* **549**, 74–77 (2017).
40. Sofia Varela, A. *et al.* CO 2 Electroreduction on Well-Defined Bimetallic Surfaces: Cu Overlayers on Pt(111) and Pt(211). *The Journal of Physical Chemistry C* (2013).
41. Simon, G. H., Kley, C. S. & Roldan Cuenya, B. Potential-Dependent Morphology of Copper Catalysts During CO2 Electroreduction Revealed by In Situ Atomic Force Microscopy. *Angewandte Chemie International Edition* **60**, 2561–2568 (2021).
42. Geri, J. B., Shanahan, J. P. & Szymczak, N. K. Testing the Push-Pull Hypothesis: Lewis Acid Augmented N2 Activation at Iron. *J Am Chem Soc* **139**, 5952–5956 (2017).
43. Dance, I. The controlled relay of multiple protons required at the active site of nitrogenase. *Dalton Transactions* **41**, 7647–7659 (2012).
44. Durrant, M. C. Controlled protonation of iron–molybdenum cofactor by nitrogenase : a structural and theoretical analysis. *Biochem. J.* **576**, 569–576 (2001).
45. McWilliams, S. F. & Holland, P. L. Dinitrogen Binding and Cleavage by Multinuclear Iron Complexes. *Accounts of Chemical Research* **48**, 2059–2065 (2015).
46. Back, S. & Jung, Y. On the mechanism of electrochemical ammonia synthesis on the Ru catalyst. *Physical Chemistry Chemical Physics* **18**, 9161–9166 (2016).
47. Skúlason, E. *et al.* A theoretical evaluation of possible transition metal electro-catalysts for N2 reduction. *Physical Chemistry Chemical Physics* **14**, 1235–1245 (2012).
48. Tsuprun, V. L. *et al.* Electron microscopy of the Mo-Fe-protein from Azotobacter vinelandii nitrogenase. *European Journal of Biochemistry* **149**, 389–392 (1985).
49. Morrison, C. N., Hoy, J. A., Zhang, L., Einsle, O. & Rees, D. C. Substrate Pathways in the nitrogenase MoFe protein by experimental identification of small molecule binding sites. *Biochemistry* **54**, 2052–2060 (2015).
50. Spatzal, T. *et al.* Nitrogenase FeMoco investigated by spatially resolved anomalous dispersion refinement. *Nature Communications* **7**, 10902 (2016).
51. Burgess, B. K. & Lowe, D. J. Mechanism of molybdenum nitrogenase. *Chemical Reviews* **96**, 2983–3011 (1996).
52. Sippel, D. *et al.* A bound reaction intermediate sheds light on the mechanism of nitrogenase. *Science (1979)* **359**, 1484–1489 (2018).
53. Foster, S. L. *et al.* Catalysts for nitrogen reduction to ammonia. *Nature Catalysis* **1**, 490–500 (2018).
54. Jasniewski, A. J., Lee, C. C., Ribbe, M. W., Ribbe, M. W. & Hu, Y. Reactivity, Mechanism, and Assembly of the Alternative Nitrogenases. *Chemical Reviews* **120**, 5107–5157 (2020).
55. Bell, J., Dunford, A. J., Hollis, E. & Henderson, R. A. The role of Mo atoms in nitrogen fixation: Balancing substrate reduction and dihydrogen production. *Angewandte Chemie - International Edition* **42**, 1149–1152 (2003).
56. Harris, D. F. *et al.* Mechanism of N2 Reduction Catalyzed by Fe-Nitrogenase Involves Reductive Elimination of H2. *Biochemistry* **57**, 701–710 (2018).

57. Sippel, D. & Einsle, O. The structure of vanadium nitrogenase reveals an unusual bridging ligand. *Nature Chemical Biology* **13**, 956–960 (2017).
58. Seefeldt, L. C. *et al.* Energy Transduction in Nitrogenase. *Accounts of Chemical Research* **51**, 2179–2186 (2018).
59. Barney, B. M., Yurth, M. G., dos Santos, P. C., Dean, D. R. & Seefeldt, L. C. A substrate channel in the nitrogenase MoFe protein. *Journal of Biological Inorganic Chemistry* **14**, 1015–1022 (2009).
60. Smith, D., Danyal, K., Raugei, S. & Seefeldt, L. C. Substrate channel in nitrogenase revealed by a molecular dynamics approach. *Biochemistry* **53**, 2278–2285 (2014).
61. Dance, I. The pathway for serial proton supply to the active site of nitrogenase: Enhanced density functional modeling of the Grotthuss mechanism. *Dalton Transactions* **44**, 18167–18186 (2015).
62. Dance, I. Computational Investigations of the Chemical Mechanism of the Enzyme Nitrogenase. *ChemBioChem* **21**, 1671–1709 (2020).
63. Lowe, D. J. & Thorneley, R. N. The mechanism of Klebsiella pneumoniae nitrogenase action. Pre-steady-state kinetics of H2 formation. *Biochem J* **224**, 877–886 (1984).
64. Thorneley, R. N., Lowe, D. J., Eday, R. R. & Miller, R. W. The coupling of electron transfer in nitrogenase to the hydrolysis of magnesium adenosine triphosphate. *Biochem Soc Trans* **7**, 633–636 (1979).
65. Seefeldt, L. C. *et al.* Control of electron transfer in nitrogenase. *Current Opinion in Chemical Biology* **47**, 54–59 (2018).
66. Yang, Z. Y. *et al.* Evidence That the Pi Release Event Is the Rate-Limiting Step in the Nitrogenase Catalytic Cycle. *Biochemistry* **55**, 3625–3635 (2016).
67. Harris, D. F., Yang, Z. Y., Dean, D. R., Seefeldt, L. C. & Hoffman, B. M. Kinetic Understanding of N2 Reduction versus H2 Evolution at the E4(4H) Janus State in the Three Nitrogenases. *Biochemistry* **57**, 5706–5714 (2018).
68. Imlay, J. A. Iron-sulphur clusters and the problem with oxygen. *Molecular Microbiology* **59**, 1073–1082 (2006).
69. Milton, R. D. *et al.* The in Vivo Potential-Regulated Protective Protein of Nitrogenase in Azotobacter vinelandii Supports Aerobic Bioelectrochemical Dinitrogen Reduction in Vitro. *J Am Chem Soc* **139**, 9044–9052 (2017).
70. Raugei, S., Seefeldt, L. C. & Hoffman, B. M. Critical computational analysis illuminates the reductive-elimination mechanism that activates nitrogenase for N2 reduction. *Proc Natl Acad Sci U S A* **115**, E10521–E10530 (2018).
71. Simpson, F. B. & Burris, R. H. A Nitrogen Pressure of 50 Atmospheres Does Not Prevent Evolution of Hydrogen by Nitrogenase. *Science (1979)* **224**, 1095–1098 (1984).
72. Lukoyanov, D., Yang, Z. Y., Dean, D. R., Seefeldt, L. C. & Hoffman, B. M. Is Mo involved in hydride binding by the four-electron reduced (E 4) intermediate of the nitrogenase MoFe protein? *J Am Chem Soc* **132**, 2526–2527 (2010).
73. Hoeke, V. *et al.* High-Resolution ENDOR Spectroscopy Combined with Quantum Chemical Calculations Reveals the Structure of Nitrogenase Janus Intermediate E4(4H). *J Am Chem Soc* **141**, 11984–11996 (2019).
74. Lukoyanov, D. *et al.* A confirmation of the quench-cryoannealing relaxation protocol for identifying reduction states of freeze-trapped nitrogenase intermediates. *Inorganic Chemistry* **53**, 3688–3693 (2014).

75. Buscagan, T. M. & Rees, D. C. Rethinking the Nitrogenase Mechanism: Activating the Active Site. *Joule* **3**, 2662–2678 (2019).
76. Schrock, R. R. Reduction of dinitrogen. *Proc Natl Acad Sci U S A* **103**, 17087 (2006).
77. Allen, B. A. D. & Senoff, C. v. Nitrogenopentammineruthenium (11) Complexes. 1964–1965 (1965).
78. Arashiba, K., Miyake, Y. & Nishibayashi, Y. A molybdenum complex bearing PNP-type pincer ligands leads to the catalytic reduction of dinitrogen into ammonia. *Nature Chemistry* **3**, 120–125 (2011).
79. Kuriyama, S. *et al.* Catalytic formation of ammonia from molecular dinitrogen by use of dinitrogen-bridged dimolybdenum-dinitrogen complexes bearing pnp-pincer ligands: Remarkable effect of substituent at pnp-pincer ligand. *J Am Chem Soc* **136**, 9719–9731 (2014).
80. Kuriyama, S. *et al.* Nitrogen fixation catalyzed by ferrocene-substituted dinitrogen-bridged dimolybdenum-dinitrogen complexes: Unique behavior of ferrocene moiety as redox active site. *Chemical Science* **6**, 3940–3951 (2015).
81. Sekiguchi, Y. *et al.* Synthesis and reactivity of iron–dinitrogen complexes bearing anionic methyl- and phenyl-substituted pyrrole-based PNP-type pincer ligands toward catalytic nitrogen fixation. *Chemical Communications* **53**, 12040–12043 (2017).
82. Eizawa, A. *et al.* Remarkable catalytic activity of dinitrogen-bridged dimolybdenum complexes bearing NHC-based PCP-pincer ligands toward nitrogen fixation. *Nature Communications* **8**, (2017).
83. Eizawa, A. *et al.* Catalytic Reactivity of Molybdenum–Trihalide Complexes Bearing PCP-Type Pincer Ligands. *Chemistry - An Asian Journal* **14**, 2091–2096 (2019).
84. Anderson, J. S., Rittle, J. & Peters, J. C. Catalytic conversion of nitrogen to ammonia by an iron model complex. *Nature* **501**, 84–87 (2013).
85. Chalkley, M. J., Castillo, T. J. del, Matson, B. D., Roddy, J. P. & Peters, J. C. Catalytic N2-to-NH3 Conversion by Fe at Lower Driving Force: A Proposed Role for Metallocene-Mediated PCET. *ACS Central Science* **3**, 217–223 (2017).
86. Kuriyama, S. *et al.* Catalytic transformation of dinitrogen into ammonia and hydrazine by iron-dinitrogen complexes bearing pincer ligand. *Nature Communications* **7**, 4–6 (2016).
87. del Castillo, T. J., Thompson, N. B., Suess, D. L. M., Ung, G. & Peters, J. C. Evaluating Molecular Cobalt Complexes for the Conversion of N2 to NH3. *Inorganic Chemistry* **54**, 9256–9262 (2015).
88. Nishibayashi, Y. Development of catalytic nitrogen fixation using transition metal-dinitrogen complexes under mild reaction conditions. *Dalton Transactions* **47**, 11290–11297 (2018).
89. Fajardo, J. & Peters, J. C. Catalytic Nitrogen-to-Ammonia Conversion by Osmium and Ruthenium Complexes. *J Am Chem Soc* **139**, 16105–16108 (2017).
90. Chalkley, M. J. & Peters, J. C. Relating N–H Bond Strengths to the Overpotential for Catalytic Nitrogen Fixation. *European Journal of Inorganic Chemistry* **2020**, 1353–1357 (2020).
91. Studt, F. & Tuczek, F. Energetics and mechanism of a room-temperature catalytic process for ammonia synthesis (schrock cycle): Comparison with biological nitrogen fixation. *Angewandte Chemie - International Edition* **44**, 5639–5642 (2005).
92. Schrock, R. R. Catalytic reduction of dinitrogen to ammonia at a single molybdenum center. *Accounts of Chemical Research* **38**, 955–962 (2005).

93. Zhang, L. *et al.* A theoretical study of the effect of a non-aqueous proton donor on electrochemical ammonia synthesis. *Physical Chemistry Chemical Physics* **20**, 4982–4989 (2018).
94. Chalkley, M. J., Castillo, T. J. del, Matson, B. D. & Peters, J. C. Fe-Mediated Nitrogen Fixation with a Metallocene Mediator: Exploring pKa Effects and Demonstrating Electrocatalysis. *J Am Chem Soc* **140**, 6122–6129 (2018).
95. Hill, P. J., Doyle, L. R., Crawford, A. D., Myers, W. K. & Ashley, A. E. Selective Catalytic Reduction of N 2 to N 2 H 4 by a Simple Fe Complex. *J Am Chem Soc* **2**, 4–7 (2016).
96. Doyle, L. R., Hill, P. J., Wildgoose, G. G. & Ashley, A. E. Teaching old compounds new tricks: efficient N2 fixation by simple Fe(N2)(diphosphine)2 complexes. *Dalton Transactions* **45**, 7550–7554 (2016).
97. Arashiba, K. *et al.* Catalytic nitrogen fixation via direct cleavage of nitrogen-nitrogen triple bond of molecular dinitrogen under ambient reaction conditions. *Bull Chem Soc Jpn* **90**, 1111–1118 (2017).
98. Kolmar, S. S. & Mayer, J. M. SmI2(H2O)n Reduction of Electron Rich Enamines by Proton-Coupled Electron Transfer. *J Am Chem Soc* **2**, (2017).
99. Roux, Y., Duboc, C. & Gennari, M. Molecular Catalysts for N2 Reduction : State of the Art , Mechanism , and Challenges. *ChemPh* **18**, 2606–2617 (2017).
100. Ashida, Y. & Nishibayashi, Y. Catalytic conversion of nitrogen molecule into ammonia using molybdenum complexes under ambient reaction conditions. *Chemical Communications* **57**, 1176–1189 (2021).
101. Burford, R. J. & Fryzuk, M. D. Examining the relationship between coordination mode and reactivity of dinitrogen. *Nature Reviews Chemistry* **1**, 26 (2017).
102. Jia, H. P. & Quadrelli, E. A. Mechanistic aspects of dinitrogen cleavage and hydrogenation to produce ammonia in catalysis and organometallic chemistry: Relevance of metal hydride bonds and dihydrogen. *Chemical Society Reviews* **43**, 547–564 (2014).
103. W. Weare, W., R. Schrock, R., S. Hock, A. & Müller, P. Synthesis of Molybdenum Complexes that Contain “Hybrid” Triamidoamine Ligands, [(Hexaisopropylterphenyl-NCH2CH2)2NCH2CH2N-aryl]3-, and Studies Relevant to Catalytic Reduction of Dinitrogen. *Inorganic Chemistry* **45**, 9185–9196 (2006).
104. Asay, M. & Morales-Morales, D. Non-symmetric pincer ligands: complexes and applications in catalysis. *Dalton Transactions* **44**, 17432–17447 (2015).
105. Rakowski DuBois, M. & DuBois, D. L. The roles of the first and second coordination spheres in the design of molecular catalysts for H2 production and oxidation. *Chemical Society Reviews* **38**, 62–72 (2009).
106. D. Wilson, A. *et al.* Hydrogen Oxidation and Production Using Nickel-Based Molecular Catalysts with Positioned Proton Relays. *J Am Chem Soc* **128**, 358–366 (2005).
107. W. Raebiger, J. *et al.* Using Ligand Bite Angles To Control the Hydricity of Palladium Diphosphine Complexes. *J Am Chem Soc* **126**, 5502–5514 (2004).
108. Macleod, K. C. & Holland, P. L. Recent developments in the homogeneous reduction of dinitrogen by molybdenum and iron K. Cory MacLeod and Patrick L. Holland* The. *Nature Publishing Group* **5**, 559–565 (2013).
109. Ung, G. & Peters, J. C. Low-Temperature N 2 Binding to Two-Coordinate L 2 Fe 0 Enables Reductive Trapping of L 2 FeN 2 − and NH 3 Generation. *Angewandte Chemie International Edition* **54**, n/a-n/a (2014).

110. Askevold, B. *et al.* Ammonia formation by metal–ligand cooperative hydrogenolysis of a nitrido ligand. *Nature Chemistry* **3**, 532–537 (2011).
111. Bagger, A., Wan, H., Stephens, I. E. L. & Rossmeisl, J. Role of Catalyst in Controlling N 2 Reduction Selectivity: A Unified View of Nitrogenase and Solid Electrodes . *ACS Catalysis* 6596–6601 (2021) doi:10.1021/acscatal.1c01128.
112. Suryanto, B. H. R. *et al.* Challenges and prospects in the catalysis of electroreduction of nitrogen to ammonia. *Nature Catalysis* **2**, 290–296 (2019).
113. Montoya, J. H., Tsai, C., Vojvodic, A. & Nørskov, J. K. The challenge of electrochemical ammonia synthesis: A new perspective on the role of nitrogen scaling relations. *ChemSusChem* **8**, 2180–2186 (2015).
114. Varley, J. B., Wang, Y., Chan, K., Studt, F. & Nørskov, J. K. Mechanistic insights into nitrogen fixation by nitrogenase enzymes. *Physical Chemistry Chemical Physics* **17**, 29541–29547 (2015).
115. Abghoui, Y. & Skúlason, E. Electrochemical synthesis of ammonia via Mars-van Krevelen mechanism on the (111) facets of group III–VII transition metal mononitrides. *Catalysis Today* **286**, 78–84 (2017).
116. Abghoui, Y. & Skúlason, E. Onset potentials for different reaction mechanisms of nitrogen activation to ammonia on transition metal nitride electro-catalysts. *Catalysis Today* **286**, 69–77 (2017).
117. Abghoui, Y., Garden, A. L., Howalt, J. G., Vegge, T. & Skúlason, E. Electroreduction of N2 to Ammonia at Ambient Conditions on Mononitrides of Zr, Nb, Cr, and V: A DFT Guide for Experiments. *ACS Catalysis* **6**, 635–646 (2016).
118. Abghoui, Y. & Skúlason, E. Transition metal nitride catalysts for electrochemical reduction of nitrogen to ammonia at ambient conditions. *Procedia Computer Science* **51**, 1897–1906 (2015).
119. Abghoui, Y. & Skúlason, E. Computational Predictions of Catalytic Activity of Zincblende (110) Surfaces of Metal Nitrides for Electrochemical Ammonia Synthesis. *The Journal of Physical Chemistry C* **121**, 6141–6151 (2017).
120. Abghoui, Y. *et al.* Enabling electrochemical reduction of nitrogen to ammonia at ambient conditions through rational catalyst design. *Physical Chemistry Chemical Physics* **17**, 4909–4918 (2015).
121. Pedersen, A. *et al.* Dual-Metal Atom Electrocatalysts: Theory, Synthesis, Characterization, and Applications. *Advanced Energy Materials* **12**, 2102715 (2022).
122. Singh, A. R. *et al.* Computational Design of Active Site Structures with Improved Transition-State Scaling for Ammonia Synthesis. *ACS Catalysis* **8**, 4017–4024 (2018).
123. Lv, X., Wei, W., Huang, B., Dai, Y. & Frauenheim, T. High-Throughput Screening of Synergistic Transition Metal Dual-Atom Catalysts for Efficient Nitrogen Fixation. *Nano Letters* **21**, 1871–1878 (2021).
124. Zhang, J. *et al.* Supported dual-atom catalysts: Preparation, characterization, and potential applications. *Chinese Journal of Catalysis* **41**, 783–798 (2020).
125. Sun, C. N., Wang, Z. L., Lang, X.-Y., Wen, Z. & Jiang, Q. Synergistic Effect of Active Sites of Double-Atom Catalysts for Nitrogen Reduction Reaction. *ChemSusChem* **n/a**, (2021).
126. Hu, B., Hu, M., Seefeldt, L. & Liu, T. L. Electrochemical Dinitrogen Reduction to Ammonia by Mo2N: Catalysis or Decomposition? *ACS Energy Letters* **4**, 1053–1054 (2019).

127. Du, H. L., Gengenbach, T. R., Hodgetts, R., Macfarlane, D. R. & Simonov, A. N. Critical Assessment of the Electrocatalytic Activity of Vanadium and Niobium Nitrides toward Dinitrogen Reduction to Ammonia. *ACS Sustainable Chemistry and Engineering* **7**, 6839–6850 (2019).
128. Kreider, M. E. *et al.* Nitride or Oxynitride? Elucidating the Composition-Activity Relationships in Molybdenum Nitride Electrocatalysts for the Oxygen Reduction Reaction. *Chemistry of Materials* (2020) doi:10.1021/acs.chemmater.9b05212.
129. Luo, J. *et al.* Limitations and Improvement Strategies for Early-Transition-Metal Nitrides as Competitive Catalysts toward the Oxygen Reduction Reaction. *ACS Catalysis* **6**, (2016).
130. Moltved, K. A. & Kepp, K. P. The Chemical Bond between Transition Metals and Oxygen: Electronegativity, d - Orbital E ffects, and Oxophilicity as Descriptors of Metal − Oxygen Interactions. *The Journal of Physical Chemistry C* **123**, (2019).
131. Karapinar, D. *et al.* Electroreduction of CO2 on Single-Site Copper-Nitrogen-Doped Carbon Material: Selective Formation of Ethanol and Reversible Restructuration of the Metal Sites. *Angewandte Chemie International Edition* **58**, 15098–15103 (2019).
132. Gu, J., Hsu, C.-S., Bai, L., Chen, H. M. & Hu, X. Atomically dispersed Fe3+ sites catalyze efficient CO2 electroreduction to CO. *Science (1979)* **364**, 1091 LP – 1094 (2019).
133. Greenlee, L. F., Renner, J. N. & Foster, S. L. The Use of Controls for Consistent and Accurate Measurements of Electrocatalytic Ammonia Synthesis from Dinitrogen. *ACS Catalysis* **8**, 7820–7827 (2018).
134. Singh, A. R. *et al.* Strategies toward Selective Electrochemical Ammonia Synthesis. *ACS Catalysis* **9**, 8316–8324 (2019).
135. Westhead, O., Jervis, R. & Stephens, I. E. L. Is lithium the key for nitrogen electroreduction? *Science (1979)* **372**, 1149–1150 (2021).
136. Rod, T. H. & Nørskov, J. K. Modeling the nitrogenase FeMo cofactor. *J Am Chem Soc* **122**, 12751–12763 (2000).
137. Li, K. *et al.* Enhancement of lithium-mediated ammonia synthesis by addition of oxygen. *Science (1979)* **1597**, 1593–1597 (2021).
138. Li, K. *et al.* Increasing Current Density of Li-Mediated Ammonia Synthesis with High Surface Area Copper Electrodes. (2022) doi:10.1021/acsenergylett.1c02104.
139. Lazouski, N., Schiffer, Z. J., Williams, K. & Manthiram, K. Understanding Continuous Lithium-Mediated Electrochemical Nitrogen Reduction. *Joule* **3**, 1127–1139 (2019).
140. Suryanto, B. H. R. *et al.* Nitrogen reduction to ammonia at high efficiency and rates based on a phosphonium proton shuttle. *Science (1979)* **372**, 1187–1191 (2021).
141. Du, H.-L. *et al.* Electroreduction of nitrogen at almost 100% current-to-ammonia efficiency. *Nature* (2022) doi:10.1038/s4158602205108y.
142. Schwalbe, J. A. *et al.* A Combined Theory-Experiment Analysis of the Surface Species in Lithium-Mediated NH3 Electrosynthesis. *ChemElectroChem* 1–9 (2020) doi:10.1002/celc.201902124.
143. Cai, X. *et al.* Lithium-mediated electrochemical nitrogen reduction: mechanistic insights to enhance performance. *iScience* 103105 (2021) doi:https://doi.org/10.1016/j.isci.2021.103105.
144. Goodenough, J. B. & Kim, Y. Challenges for rechargeable Li batteries. *Chemistry of Materials* **22**, 587–603 (2010).
145. Goodenough, J. B. & Park, K. S. The Li-ion rechargeable battery: A perspective. *J Am Chem Soc* **135**, 1167–1176 (2013).

146. Xu, K. Nonaqueous liquid electrolytes for lithium-based rechargeable batteries. *Chemical Reviews* **104**, 4303–4417 (2004).
147. Zhou, Y. *et al.* Real-time mass spectrometric characterization of the solid–electrolyte interphase of a lithium-ion battery. *Nature Nanotechnology* **15**, 224–230 (2020).
148. Peled, E. The Electrochemical Behavior of Alkali and Alkaline Earth Metals in Nonaqueous Battery Systems—The Solid Electrolyte Interphase Model. *Journal of The Electrochemical Society* **126**, 2047 (1979).
149. Verma, P., Maire, P. & Novák, P. A review of the features and analyses of the solid electrolyte interphase in Li-ion batteries. *Electrochimica Acta* **55**, 6332–6341 (2010).
150. Heiskanen, S. K., Kim, J. & Lucht, B. L. Generation and Evolution of the Solid Electrolyte Interphase of Lithium-Ion Batteries. *Joule* **3**, 2322–2333 (2019).
151. Peled, E. & Menkin, S. Review—SEI: Past, Present and Future. *Journal of The Electrochemical Society* **164**, A1703–A1719 (2017).
152. Castelli, I. E. *et al.* The role of an interface in stabilizing reaction intermediates for hydrogen evolution in aprotic electrolytes. *Chemical Science* **11**, 3914–3922 (2020).
153. Gauthier, M. *et al.* Electrode-Electrolyte Interface in Li-Ion Batteries: Current Understanding and New Insights. *Journal of Physical Chemistry Letters* **6**, 4653–4672 (2015).
154. Xiong, R., Pan, Y., Shen, W., Li, H. & Sun, F. Lithium-ion battery aging mechanisms and diagnosis method for automotive applications: Recent advances and perspectives. *Renewable and Sustainable Energy Reviews* **131**, 110048 (2020).
155. Zhang, Z. *et al.* Operando Electrochemical Atomic Force Microscopy of Solid-Electrolyte Interphase Formation on Graphite Anodes: The Evolution of SEI Morphology and Mechanical Properties. *ACS Applied Materials & Interfaces* (2020) doi:10.1021/acsami.0c11190.
156. Krishnamurthy, D., Lazouski, N., Gala, M. L., Manthiram, K. & Viswanathan, V. Closed-Loop Electrolyte Design for Lithium-Mediated Ammonia Synthesis. *ACS Central Science* **7**, 2073–2082 (2021).
157. Mogensen, R., Brandell, D. & Younesi, R. Solubility of the Solid Electrolyte Interphase (SEI) in Sodium Ion Batteries. *ACS Energy Letters* (2016) doi:10.1021/acsenergylett.6b00491.
158. Strmcnik, D. *et al.* Electrocatalytic transformation of HF impurity to H2 and LiF in lithium-ion batteries. *Nature Catalysis* **1**, 255–262 (2018).
159. Fears, T. M. *et al.* Evaluating the solid electrolyte interphase formed on silicon electrodes: A comparison of: Ex situ X-ray photoelectron spectroscopy and in situ neutron reflectometry. *Physical Chemistry Chemical Physics* **18**, 13927–13940 (2016).
160. Zhang, Y. *et al.* Revealing electrolyte oxidation: Via carbonate dehydrogenation on Ni-based oxides in Li-ion batteries by in situ Fourier transform infrared spectroscopy. *Energy and Environmental Science* **13**, 183–199 (2020).
161. Hy, S. *et al.* In situ surface enhanced Raman spectroscopic studies of solid electrolyte interphase formation in lithium ion battery electrodes. *Journal of Power Sources* **256**, 324–328 (2014).
162. Lazouski, N. *et al.* Proton Donors Induce a Differential Transport Effect for Selectivity toward Ammonia in Lithium-Mediated Nitrogen Reduction. *ACS Catalysis* 5197–5208 (2022) doi:10.1021/acscatal.2c00389.

163. McEnaney, J. M. *et al.* Ammonia synthesis from N2 and H2O using a lithium cycling electrification strategy at atmospheric pressure. *Energy and Environmental Science* **10**, 1621–1630 (2017).
164. Kim, K. *et al.* Electrochemical Synthesis of Ammonia from Water and Nitrogen: A Lithium-Mediated Approach Using Lithium-Ion Conducting Glass Ceramics. *ChemSusChem* **11**, 120–124 (2018).
165. Kim, K., Chen, Y., Han, J. I., Yoon, H. C. & Li, W. Lithium-mediated ammonia synthesis from water and nitrogen: A membrane-free approach enabled by an immiscible aqueous/organic hybrid electrolyte system. *Green Chemistry* **21**, 3839–3845 (2019).
166. del Castillo, T. J., Thompson, N. B. & Peters, J. C. A Synthetic Single-Site Fe Nitrogenase: High Turnover, Freeze-Quench 57Fe Mössbauer Data, and a Hydride Resting State. *J Am Chem Soc* **138**, 5341–5350 (2016).
167. Tanaka, H. *et al.* Unique behaviour of dinitrogen-bridged dimolybdenum complexes bearing pincer ligand towards catalytic formation of ammonia. *Nature Communications* **5**, (2014).
168. Kuriyama, S. *et al.* Direct Transformation of Molecular Dinitrogen into Ammonia Catalyzed by Cobalt Dinitrogen Complexes Bearing Anionic PNP Pincer Ligands. *Angewandte Chemie - International Edition* **55**, 14291–14295 (2016).
169. Tanaka, H., Nishibayashi, Y. & Yoshizawa, K. Interplay between Theory and Experiment for Ammonia Synthesis Catalyzed by Transition Metal Complexes. *Accounts of Chemical Research* **49**, 987–995 (2016).
170. Higuchi, J. *et al.* Preparation and reactivity of iron complexes bearing anionic carbazole-based PNP-type pincer ligands toward catalytic nitrogen fixation. *Dalton Transactions* **47**, 1117–1121 (2018).
171. Milton, R. D. & Minteer, S. D. Nitrogenase Bioelectrochemistry for Synthesis Applications. *Accounts of Chemical Research* **52**, 3351–3360 (2019).
172. Wolfschmidt, H. *et al.* STM, SECPM, AFM and Electrochemistry on Single Crystalline Surfaces. *Materials* **3**, 4196–4213 (2010).
173. Simon, H. M., Gosink, M. M., Roberts, G. P., Al, S. E. T. & Acteriol, J. B. Importance of cis Determinants and Nitrogenase Activity in Regulated Stability of the Klebsiella pneumoniae Nitrogenase Structural Gene mRNA. *Journal of Bacteriology* **181**, 3751–3760 (1999).
174. Lukoyanov, D., Barney, B. M., Dean, D. R., Seefeldt, L. C. & Hoffman, B. M. Connecting nitrogenase intermediates with the kinetic scheme for N2 reduction by a relaxation protocol and identification of the N2 binding state. *Proc Natl Acad Sci U S A* **104**, 1451–5 (2007).
175. M. Barney, B. *et al.* Diazene (HNNH) Is a Substrate for Nitrogenase: Insights into the Pathway of N2 Reduction. *Biochemistry* **46**, 6784–6794 (2007).
176. Hinnemann, B. & Nørskov, J. K. Catalysis by Enzymes: The Biological Ammonia Synthesis. *Topics in Catalysis* **37**, 55–70 (2006).
177. Varghese, F. *et al.* A low-potential terminal oxidase associated with the irononly nitrogenase from the nitrogen-fixing bacterium Azotobacter vinelandii. *Journal of Biological Chemistry* **294**, 9367–9376 (2019).

[H1] Highlighted references

Singh, A. R. *et al.* Electrochemical Ammonia Synthesis—The Selectivity Challenge. *ACS Catalysis* **7**, 706–709 (2017).
This was the first paper to provide a unified kinetic model to understand N_2 reduction and selectivity in homogeneous catalysts, nitrogenase and solid electrocatalysts.

Chalkley, M. J., Drover, M. W. & Peters, J. C. Catalytic N 2 -to-NH 3 (or -N 2 H 4) Conversion by Well-Defined Molecular Coordination Complexes. *Chemical Reviews* **120**, 5582–5636 (2020).
This comprehensive review from Chalkley et al is a useful introduction to the state-of-the-art for homogeneous nitrogen reduction to ammonia.

Einsle, O. & Rees, D. C. Structural Enzymology of Nitrogenase Enzymes. *Chemical Reviews* **120**, 4969–5004 (2020).
This comprehensive review from Einsle and Rees covers the latest understanding in the structure of the FeMo-co, as well as considering comparisons to Fe- and V-based nitrogenase.

Seefeldt, L. C. *et al.* Energy Transduction in Nitrogenase. *Accounts of Chemical Research* **51**, 2179–2186 (2018).
This work provides an in-depth study into the complex mechanism of electron transfer in nitrogenase.

Ashida, Y. & Nishibayashi, Y. Catalytic conversion of nitrogen molecule into ammonia using molybdenum complexes under ambient reaction conditions. *Chemical Communications* **57**, 1176–1189 (2021).
Ashida and Nishibayashi comprehensively discuss the various mechanisms by which Mo-based homogeneous catalysts carry out nitrogen reduction to ammonia.

Peled, E. & Menkin, S. Review—SEI: Past, Present and Future. *Journal of The Electrochemical Society* **164**, A1703–A1719 (2017).
This review by Peled and Menkin is a useful introduction to the Solid Electrolyte Interphase for those new to battery science.

Tsuneto, A., Kudo, A. & Sakata, T. Efficient Electrochemical Reduction of N 2 to NH 3 Catalyzed by Lithium . *Chemistry Letters* **22**, 851–854 (1993).
This was the original paper to discover the lithium-mediated ammonia synthesis paradigm, the only method tested by Andersen et al. that passed their rigorous protocol.

[H1] Acknowledgements

O.W. acknowledges funding from the EPSRC and SFI Centre for Doctoral Training in Advanced Characterisation of Materials Grant Ref: EP/S023259/1, J.B., I.EL.S. and M.T acknowledge funding from the National Research Council Canada through the Materials for Clean Fuels Challenge Program. I.E.L.S. acknowledges funding from the European Research Council (ERC) under the European Union's Horizon 2020 research and innovation programme (grant agreement no. 866402). AB and JR thanks the Danish National Research Foundation DNRF-149 and the Carlsberg foundation

[H1] Competing Interests Statement

The authors declare no competing interest.

[H1] Author contributions

All authors co-conceived the concept and constructed the structure for the article. O.W., J.B. and I.E.L.S. researched data for the article and wrote the initial draft. A.A., A.F., A.B. and J.R. contributed substantially to discussion of content. A.A., A.B., J.W.M., J.R., A.F., M.T. and R.J. reviewed the manuscript before submission. O.W., J.B. and I.E.L.S. edited the final version for submission.

[H1] Graphical abstract suggestion

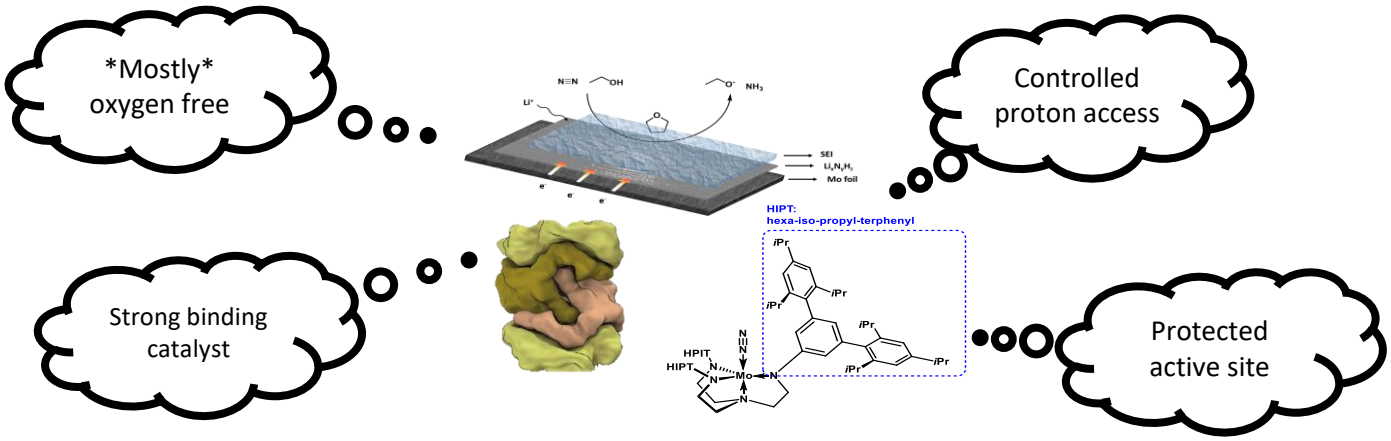

[H1] Publisher's note

Springer Nature remains neutral with regard to jurisdictional claims in published maps and institutional affiliations.

[H1] How to cite this article

Westhead, O. et al., Near ambient N2 fixation on solid electrodes versus enzymes and homogeneous catalysts, Nat. Rev. Chem. 4, xxxxx (2022).

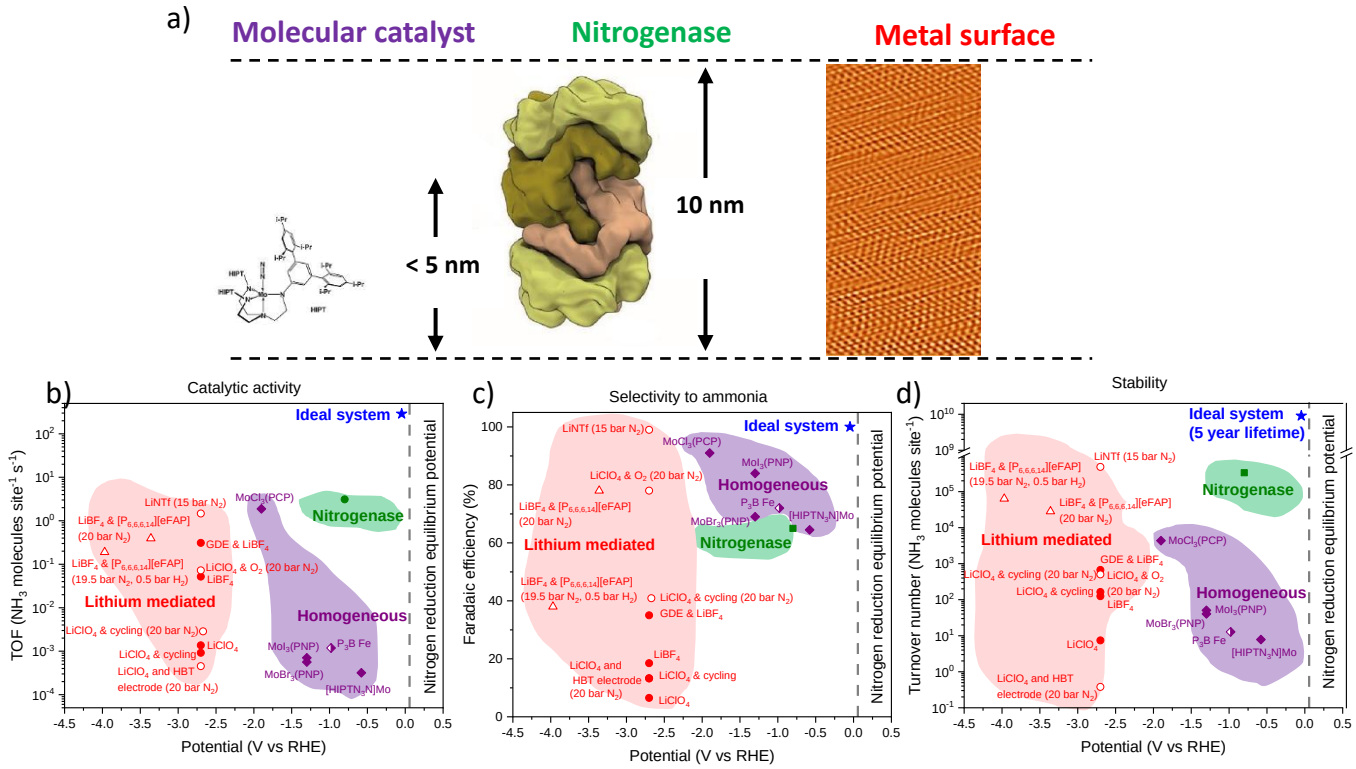

Figure 1. ***A comparison of molecular catalysts, nitrogenase and a metal surface*** *a) Image comparing the approximate footprint of the MoFe protein of the nitrogenase enzyme*[36,48]*, the Schrock catalyst*[19] *and a metallic Ru (001) surface measured by contact mode AFM*[172]*, with individually resolved atoms (approximately 10,000 active sites shown). Schrock catalyst image reproduced with permission from REF.* [19]*, American Association for the Advancement of Science. Nitrogenase image reproduced with permission from REF.* [36]*, American Chemical Society. AFM image of Ru reproduced with permission from REF.* [172]*, MDPI. b – d: Three plots to compare b) the relative turnover frequencies per active site, c) the relative Faradaic efficiences and d) the relative turnover numbers vs operating potential for lithium mediated solid electrode systems (red, circle and triangle; circle points represent experiments carried out using a sacrificial proton donor, triangle points represent experiments carried out using a recylcable proton donor) (*$LiBF_4$ *& gas diffusion electrode from Lazouski et al*[29]*,* $LiBF_4$ *from Lazouski et al*[139]*,* $LiClO_4$ *from Andersen et al*[20]*,* $LiClO_4$ *& cycling from Andersen et al*[30]*,* $LiBF_4$ *&* $[P_{6,6,6,14}][eFAP]$ *from Suryanto et al*[140]*,* $LiClO_4$ *& oxygen from Li et al*[137]*,* $LiClO_4$ *& high surface area electrode from Li et al*[138]*,* LiNTf from Du et al[141]*), four homogeneous systems (purple, rhombus) (*MoX_3*(PNP), where X= I or Br from Arashiba et al*[97]*, the Schrock catalyst (*$[HIPTN_3N]Mo$*) from Yandulov and Schrock*[19]*, the* $MoCl_3$*(PCP) catalyst using a coordinated proton donor and reducing agent from Ashida et al*[27] *and the* P_3^BFe *catalyst from Chalkley et al*[85]*) and nitrogenase (green, square) (using data from Seefeldt et al*[65]*, Rivera-Ortiz and Burris*[3]*, Simon et al*[173] *and Bukas and Norskov*[37]*). Filled points represent experiments carried out under 1 bar* N_2*. Hollow points represent experiments carried out at higher* N_2 *partial pressure. Half filled points represent experiments done at a temperature other than ambient. The blue star represents the 'ideal electrode' with 100% Faradaic efficiency, 1 A* cm^{-2} *current density, 10 mV overpotential and roughness factor 33. The dashed line is the nitrogen reduction eqilibrium potential. See Supplementary Information for calculation details. Figures b-d calculated using data from REFs.* 3,19,20,29–31,37,58,78,85,137–141,173

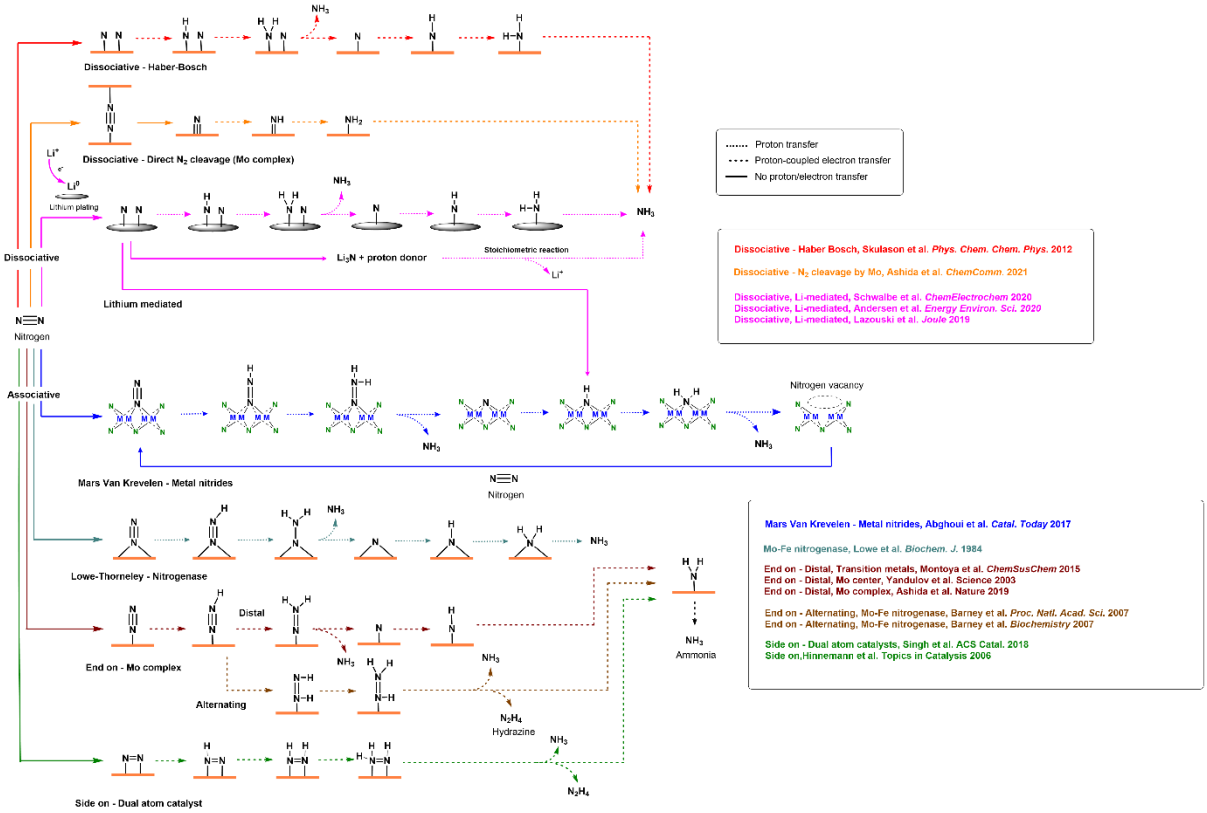

Figure 2. ***A schematic representation of the various reduction pathways through which nitrogen can be reduced to ammonia.*** *The dissociative mechanism in transition metals was adapted from Skulason et al.*[47]*, Lowe-Thorneley from Lower et al.*[63]*, dissociative mechanism in homogeneous complexes from Ashida and Nishibayshi*[100]*, end on distal from Montoya et al., Yandulov et al., and Ashida et al.* [19,31,113]*, alternating distal from Barney et al. and Lukoyanov et al*[174,175]*, side on from Singh et al. and Hinnemann et al.,* [115,122,176]*Li-mediated in Mo and Cu from Schwalbe et al. Andersen et al. and Lazouski et al*[30,139,142]*and Mars van Krevelen mechanism in metal nitrides from Abghoui et al.*[115]*.*

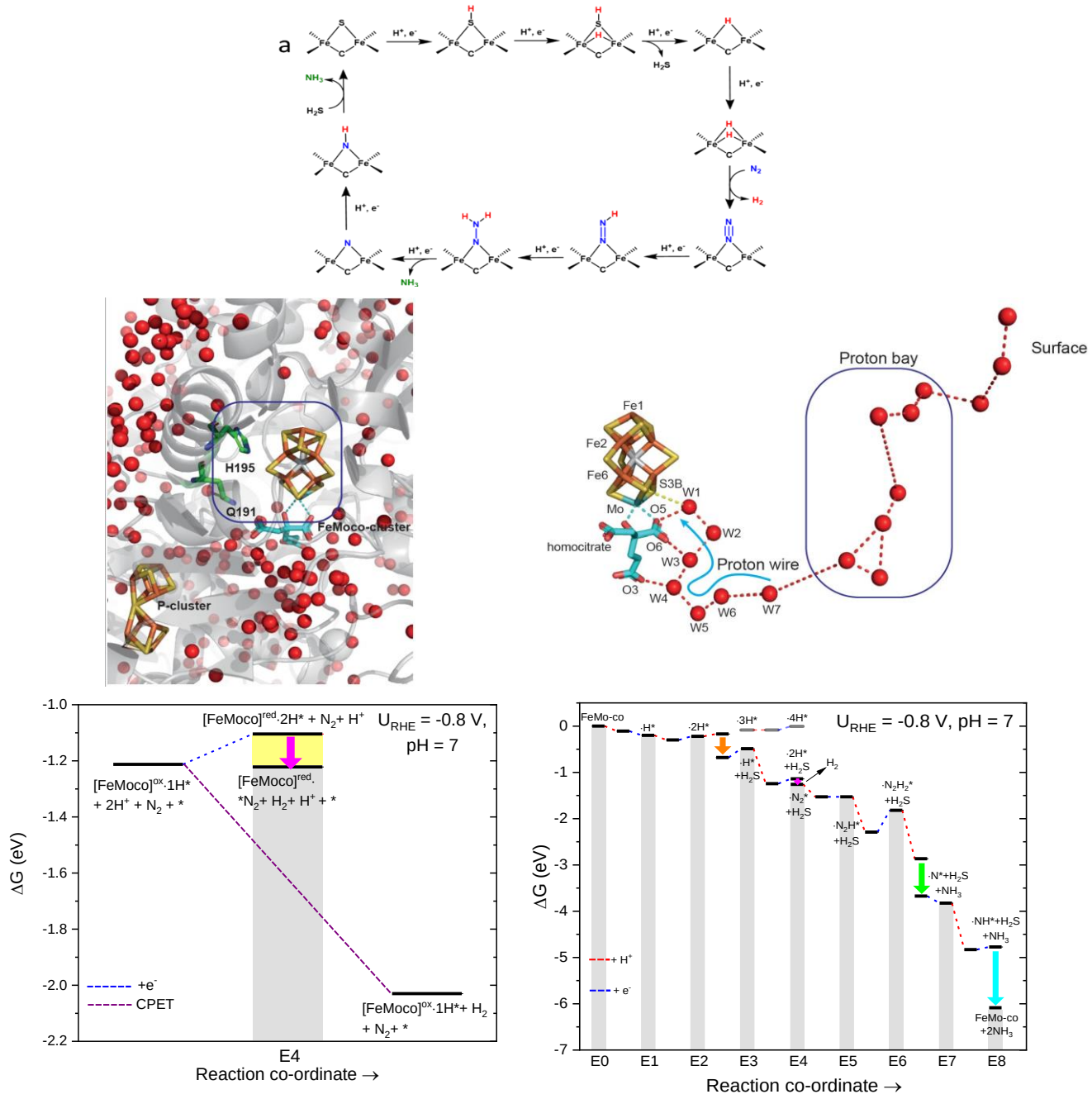

Figure 3. ***A summary of the nitrogenase reduction scheme and proton delivery mechanism*** *(a) Scheme of nitrogenase catalytic cycle. Sulfur bonded to Fe atoms is removed and replaced by hydrides which can recombine and yield H_2 in exchange for N2 (E_0-E_4). The last catalytic steps (after E_4) reduce N_2 into NH_3, whose desorption entails the incorporation of sulfur into the Fe active site*[37]*. Reproduced with permission from REF.* [37]*, arXiv. (b) A diagram of the environment surrounding the catalytic cofactor of nitrogenase, where the area within the blue rectangle does not contain any water (red dots)* [43] *. Reproduced with permission from REF.* [43]*, Royal Society of Chemistry. (c) A diagram showing the transport of protons to the active site*[43]*. Reproduced with permission from REF.* [43]*, Royal Society of Chemistry (d) A free energy diagram showing the importance of delayed charge transfer in avoiding hydrogen evolution. If proton transfer occurs via coupled proton electron transfer, the FeMo-co returns to a previous step in the reduction scheme and cannot bind N_2. If there is N_2 present and slow proton and electron transfer, the FeMo-co can bind N_2, indicated by the pink arrow. If slow proton and electron transfer occurs but there is no N_2 available, the FeMo-co also returns to the same previous step* [37]*. Adapted with permission from REF.* [37]*, arXiv. (e) A free energy diagram showing the reduction steps of the mechanism by which nitrogenase binds and activates N_2 to make NH_3*[37]*. Orange, pink, green and blue arrows show H_2S dissociation, N_2 binding, the chemical desorption of the first NH_3 molecule and the chemical*

desorption of the second NH_3 molecule, respectively. The greyed-out pathway represents the energy penalty without H_2S dissociation. Reproduced with permission from REF. [37], arXiv.

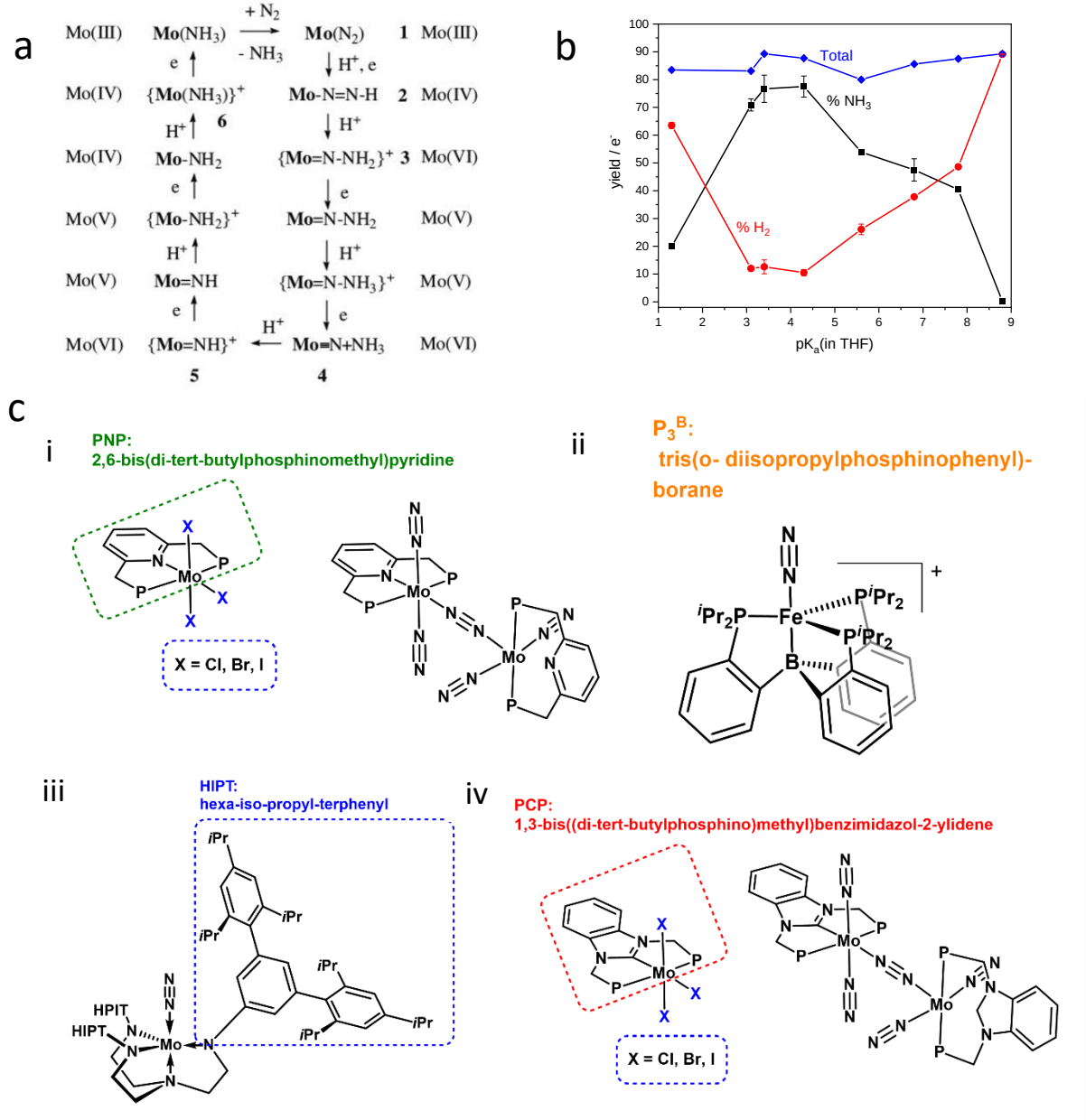

Figure 4. ***Homogeneous nitrogen reduction*** *(a) The reduction scheme proposed by Yandulov and Schrock, where protons and electrons are added to the catalyst in a stepwise fashion[19]. Reproduced with permission from REF. [19], Springer Nature Limited (b) A graph to show the relationship between the pK_a value of a proton source (various anilinium acids) in THF and the percentage yield per electron of NH_3 and H_2 for Peters and coworkers' P_3BFe^+ molecular catalyst[94]. The reducing agent used was Cp^*_2Co (54 equivalents). All tests carried out at ambient pressure and -78°C with 108 equivalents of the relevant acid used. Line added to guide the eye. Drawn using data from REF. [94]. (c) Diagrams of the molecular complexes considered in figure 1b-d: (i) MoX3(PNP), where X= I or Br from Arashiba et al[97], (ii) P_3^BFe from Chalkley et al[85], (iii) the Schrock catalyst ($[HIPTN_3N]Mo$) [19],* and (iv) *$MoCl_3$(PCP) using a coordinated proton donor and reducing agent from Ashida et al[27].*

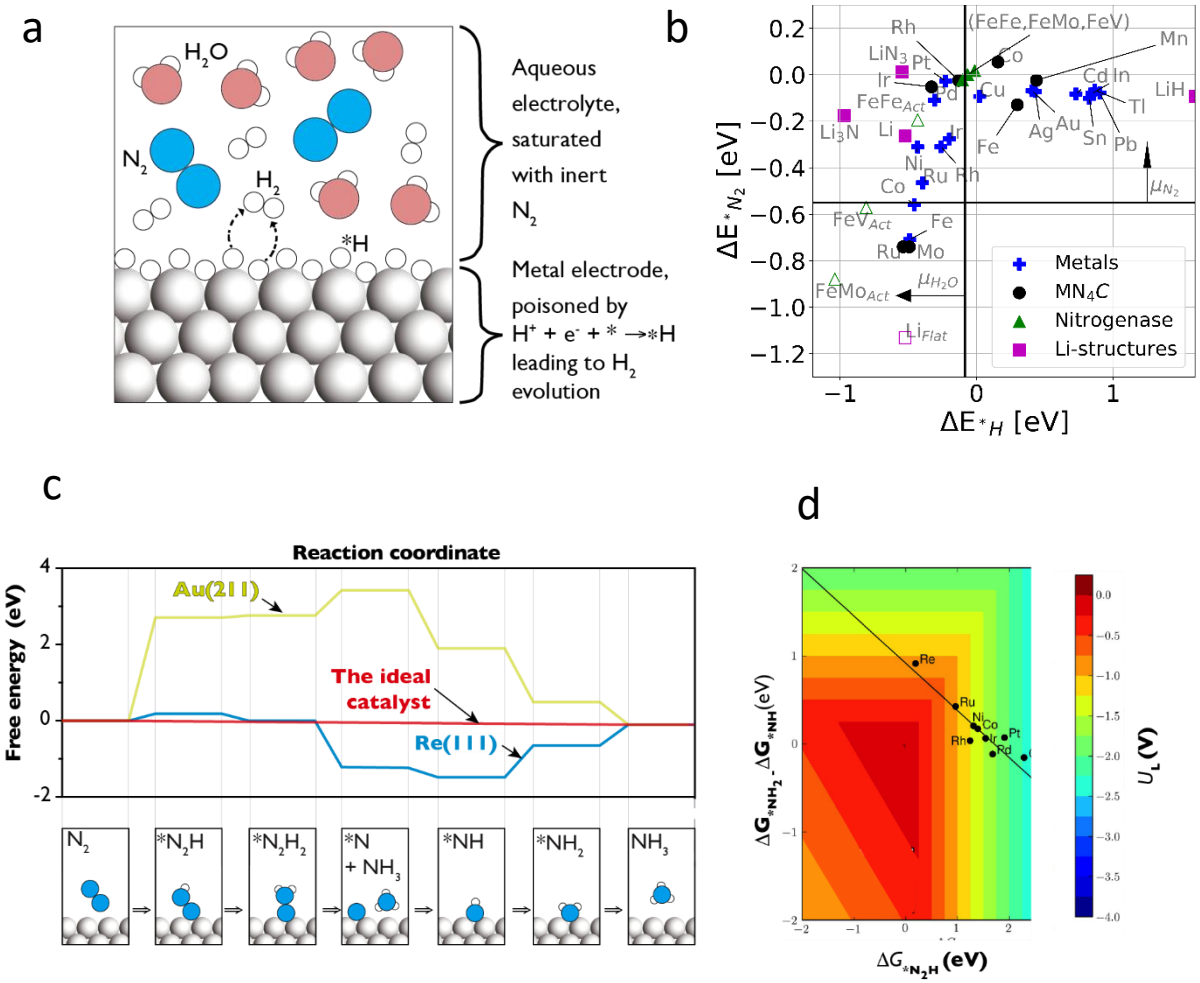

Figure 5. ***The limitations of metal electrodes in aqueous electrolytes.*** *(a) A diagram to highlight the effect of hydrogen poisoning*[9]*. Reproduced with permission from REF.* [9]*, Energy-X. (b) A classification scheme produced showing *N2 vs H* binding energies for nitrogen reduction catalysts in aqueous electrolytes at ambient temperature and pressure*[111] *. The vertical line shows 1/2H_2(g) vs H* and the horizontal line shows N_2(g) vs N_2*. Arrows show how the line would move by changing μ_{H_2O} and μ_{N_2}. Reproduced with permission from REF.* [111]*, American Chemical Society (c) A free energy diagram for the associative N_2 reduction mechanism on Ag(211), Re(111) and the ideal catalyst*[9]*. Adapted with permission from REF.* [9] *, Energy-X. (d) A volcano contour plot showing how unfavourable scaling between N-containing intermediates results in excessively negative limiting potentials, U_L to drive reaction, i.e. large overpotentials*[113]*. Reproduced from with permission from REF.* [9]*, Energy-X.*

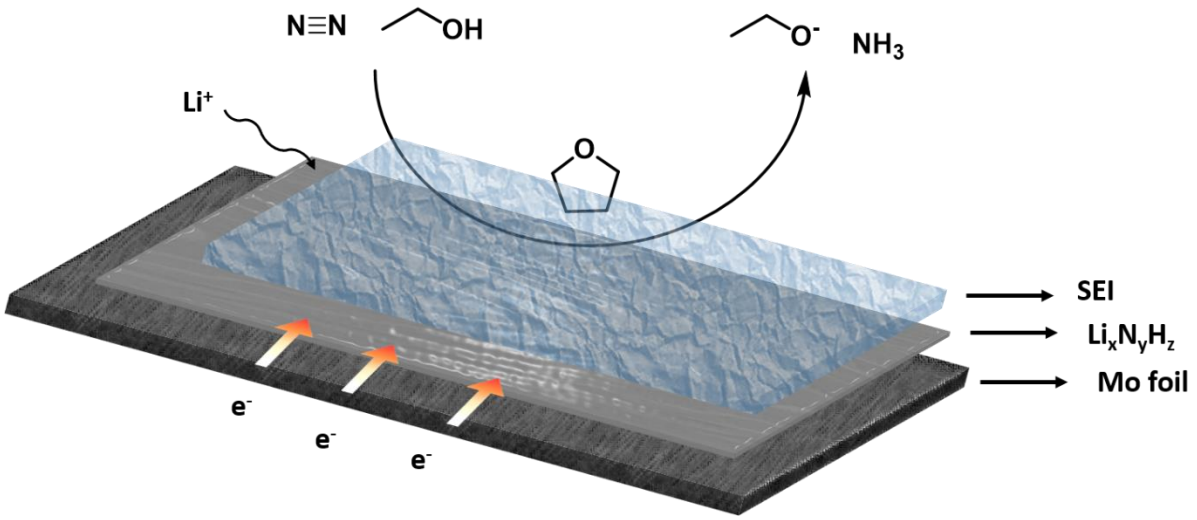

Figure 6 A schematic of the lithium mediated system, where the formed SEI restricts proton access to the electrode surface.

	Enzymes	Homogeneous	Solid Electrode
Key example	Nitrogenase	Mo-complex $[MoCl_3(PCP)]$[31]	$Li/Li_xN_yH_z$
Strongly binding active site	✓ Fe atoms [28,52]	✓ Mo[31]	✓ Li, Li_3N, LiH or mixed $Li_xN_yH_z$[30,142]
O_2-free	✓ [177]	✓ [31]	(✓) Inhibited activity in bulk O_2 but enhanced activity in trace O_2 (2021)[137]
Limited access to H^+	✓ Delivery by proton wire[43], sterically protected active site[37]	✓ Sterically protected active site, single proton and electron transfer (PCET)[31]	✓ Non-aqueous electrolyte, controlled proton donor quantities[23,139]
Limited access to e^-	✓ Limited by Pi release[27]	✓ Mild reducing agent, single proton and electron transfer (PCET)[31]	✗ Electrons freely available at electrode surface

Table 1 A table to show the differences between the lithium mediated system, homogeneous systems and nitrogenase in terms of access to reactants

[H1] ToC blurb

Green dinitrogen fixation is critical for the decarbonisation of fertilisers and fuel. This Review examines the common grounds and complementarities between catalysis using homogeneous compounds, enzymes, and solid electrodes.